The Physics of Glueballs

Vincent Mathieu
Groupe de Physique Nucléaire Théorique,
Université de Mons-Hainaut,
Académie universitaire Wallonie-Bruxelles,
Place du Parc 20, BE-7000 Mons, Belgium.
vincent.mathieu@umh.ac.be

Nikolai Kochelev
Bogoliubov Laboratory of Theoretical Physics,
Joint Institute for Nuclear Research,
Dubna, Moscow region, 141980 Russia.
kochelev@theor.jinr.ru

Vicente Vento
Departament de Física Teòrica and Institut de Física Corpuscular,
Universitat de València-CSIC,
E-46100 Burjassot (Valencia), Spain.
vicente.vento@uv.es

Glueballs are particles whose valence degrees of freedom are gluons and therefore in their description the gauge field plays a dominant role. We review recent results in the physics of glueballs with the aim set on phenomenology and discuss the possibility of finding them in conventional hadronic experiments and in the Quark Gluon Plasma. In order to describe their properties we resort to a variety of theoretical treatments which include, lattice QCD, constituent models, AdS/QCD methods, and QCD sum rules. The review is supposed to be an informed guide to the literature. Therefore, we do not discuss in detail technical developments but refer the reader to the appropriate references.

I. INTRODUCTION

Quantum Chromodynamics (QCD) is the theory of the hadronic interactions. It is an elegant theory whose full non perturbative solution has escaped our knowledge since its formulation more than 30 years ago.[1] The theory is asymptotically free[2, 3] and confining.[4] A particularly good test of our understanding of the nonperturbative aspects of QCD is to study particles where the gauge field plays a more important dynamical role than in the standard hadrons. In particular glueballs, bound states of gluons, represent such a scenario.

The glueball spectrum has attracted much attention since the early days of QCD.[5] The interest in this subject is related to the significant progress in the understanding of the properties of such states within QCD, as well as, in the new possibilities for their identification in modern experiments. Historically the investigation of the glueball properties started in the bag model by Jaffe and Johnson.[6] They found many glueball states with different quantum numbers lying in the mass interval 1000-2000 MeV. They emphasized that one should expect rather small widths for such states because their decays in conventional hadrons violate the Okubo-Zweig-Iizuka (OZI) rule.[7]

After this pioneering work the study of glueballs was carried out by using various versions of constituent models, by exploiting the QCD sum rule approach and by performing lattice QCD calculations. Glueballs have not been an easy subject to study due to the lack of phenomenological support and therefore much debate has been associated with their properties. The main achievement of these approaches is the understanding of the deep relation between the properties of the glueball states and the structure of the QCD vacuum. Besides, they provide a determination of the spectrum both in gluodynamics, the theory with just gluons and no quarks, and in QCD. However, in (unquenched) QCD, the results of several calculations for the spectrum are still not universally accepted, in particular, for the lowest lying glueballs.[8, 9]

From the phenomenological point of view it has become clear by now that it is difficult to single out which states of the hadronic spectrum are glueballs because we lack the necessary knowledge to determine their decay properties. Moreover the strong expected mixing between glueballs and quark states leads to a broadening of the possible glueball states which does not simplify their isolation. The wishful sharp resonances which would confer the glueball spectra the beauty and richness of the baryonic and mesonic spectra are lacking. This confusing picture has led to a loss of theoretical and experimental interest in these hadronic states. However, it is important to stress, that if they were to exist they would be a beautiful and unique consequence of QCD. At the present, several candidates for the low mass glueballs with quantum numbers 0^{++}, 2^{++}, 0^{-+} and 1^{--} are under discussion. [10, 11, 12, 13, 14, 15]

In this review we will discuss the modern development in glueball spectroscopy from various perspectives. In section II we will summarize the results that lattice techniques have obtained for the spectrum, both in the pure gauge theory and in the unquenched calculations. In section III we present a review on constituent models. Section IV is dedicated to discuss QCD sum rules. In section V the production and decay mechanisms of glueballs in hadronic reactions are discussed. In section VI the peculiarities of glueball production and behavior in Quark-Gluon Plasma (QGP) is considered. Section VII is dedicated to present two open topics the relation between the pomeron and glueballs and glueball-quarkonium mixing. Finally in section VIII we extract the main conclusions of our analysis and try to foresee future developments.

II. LATTICE QCD

A. Overview

Gluon self-couplings in QCD suggest the existence of glueballs, bound states of mainly gluons. Investigating glueball physics requires an intimate knowledge of the confining QCD vacuum and it is well known that such properties cannot be obtained using standard perturbative techniques. To handle the nonperturbative regime of QCD, one can resort to numerical methods, known as lattice QCD. Lattice QCD needs as input the quark masses and an overall scale, conventionally given by Λ_{QCD}. Then any Green function can be evaluated by taking average of suitable combinations of lattice fields in vacuum samples. This allows masses and matrix elements, particularly those of weak or electromagnetic currents, to be studied. One limitation of the lattice approach is in exploring hadronic decays because the lattice, using Euclidean time, has no concept of asymptotic states.

Lattice QCD was originally formulated by Wilson [4] and is a clever implementation of the QCD dynamics using a finite difference formalism. The starting point is the correlation function in a discrete Euclidean space

$$C(t) = \langle \Omega | \phi^\dagger(t)\phi(0)|\Omega\rangle \sim \int dU \int d\psi \int d\bar{\psi} \sum_{\boldsymbol{x}} \phi^\dagger(\mathbf{0},0)\phi(\boldsymbol{x},t) e^{-S_F(\beta)-S_G(\beta)}, \tag{1}$$

where S_F is the fermion action and S_G the pure gauge action. The continuum limit is controlled by the input parameter $\beta = 2N/g^2$ (N is the number of color). By varying the inverse lattice coupling β we vary the lattice spacing a. The fermion action can be integrated out exactly in Eq. (1) to produce the fermion determinant. The determinant describes the dynamics of the sea quarks. In quenched QCD calculations, the determinant is set to a constant.[16]

The physics is extracted from the fit

$$C(t) = \sum_n |\langle \Omega|\phi|n\rangle|^2 \exp(-M_n t). \tag{2}$$

$|n\rangle$ are the energy eigenstates and M_n the corresponding masses. In practice, one has to choose the operator ϕ which best overlaps with the lowest-lying glueball in the channel of interest. ϕ is thus expanded in a basis with well-defined symmetry properties under the octahedral group and the variational coefficients are determined by Monte-Carlo simulations.[17]

The spectrum in a box with periodic boundary conditions includes not only single glueball states, but also states consisting of several glueballs and torelons (gluon excitations which wrap around the toroidal lattice). Fortunately, torelons are found to overlap only weakly with single glueball states.[17, 18]

Since (classical) gluodynamics is dimensionless, its observables will be also dimensionless. Masses are usually expressed in terms of the string tension $m/\sqrt{\sigma}$ or the hadronic scale parameter $r_0 m$ defined through the static potential between quarks $[r^2 dV(r)/dr]_{r=r_0} = 1.65$.[17, 19] Their values are very close and usually read

$$\sqrt{\sigma} = 440 \pm 20 \text{ MeV}, \qquad r_0^{-1} = 410 \pm 20 \text{ MeV}. \tag{3}$$

In lattice calculations there are errors arising from the finite size of the lattice spacing a and the finite lattice volume. But for small enough a we expect the continuum limit to be approached as

$$\frac{m(a)}{\sqrt{\sigma(a)}} = \frac{m(0)}{\sqrt{\sigma(0)}} + ca^2\sigma(0), \tag{4}$$

with a constant c.[20]

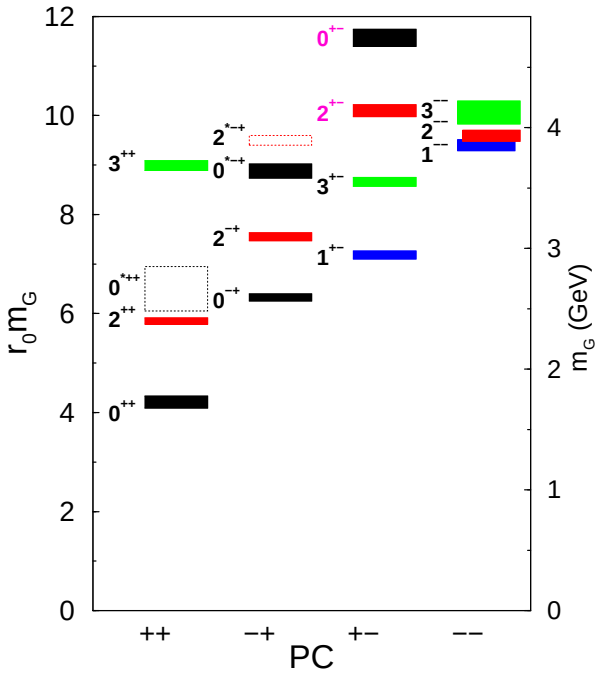

FIG. 1: The mass spectrum of glueballs in pure $SU_C(3)$ gauge theory . The masses are given in units of the hadronic scale r_0 along the left vertical axis and in GeV along the right vertical axis. The mass uncertainties indicated by the vertical extents of the boxes do not include the uncertainty in r_0. Numerical results are listed in the table below. In some cases, the spin-parity assignment for a state is not unique. The figure shows the smallest J value, the other possibilities are indicated in the second column of the table.

B. Pure gauge spectrum

The pure gauge spectrum of quenched QCD was investigated initially by Morningstar and Peardon in an anisotropic lattice.[17] They used different spacings for the spatial a_s and for the temporal a_t extensions with the ratio $\xi = a_s/a_t$. This technique allows to control better the inherent errors induced by the lattice.

Morningstar and Peardon identified 13 glueballs below 4 GeV. In order to distinguish single from multiple glueball states, they determined approximately the locations of the two-particles states using the mass estimation of the lowest few particles. In their estimates of these locations they assumed that the two glueballs do not interact and that the threshold for their production is given by the energy

$$E_{2G} \approx \sqrt{\boldsymbol{p}_1^2 + m_1^2} + \sqrt{\boldsymbol{p}_2^2 + m_2^2}, \tag{5}$$

where $\boldsymbol{p}_1 = -\boldsymbol{p}_2$ and $m_{1,2}$ are the masses of the single glueballs. All states lying below the two-glueball threshold are then single glueball states. These authors pointed out that they cannot rule out a single glueball interpretation for higher states. They do not find any hint that their states are torelon pairs.

Finite volume effects are quite under control. When going from a $6^3 \times 40$ lattice to a $8^3 \times 40$ lattice, the fractional changes on the mass $\delta = 1 - m'/m$ are less than a few percent and consistent with zero. The largest effect of these errors occur in the A_1^{*++} and T_1^{*+-} representations of the octahedral group. They are the main cause of uncertainties in the 0^{*++} and 2^{*+-} glueballs. The proximity of the two glueball thresholds and the finite volume errors on the A_1^{*++} lead the authors to withhold judgment on whether or not this level is a single glueball.

Lattice spacing errors, see Eq. (4), are expected to be $\mathcal{O}(a_t^2, a_s^4, \alpha_s a_s^2)$ from perturbation theory.[17, 21] But the results for different ξ suggest that $\mathcal{O}(a_t^2, \alpha_s a_s^2)$ errors are negligible. They extrapolate to the continuum limit assuming $\mathcal{O}(a_s^4)$. In addition to these lattice errors of the dimensionless masses $r_0 m$, one has to add the error arising from the scale parameters (3) when presenting the absolute masses.

Representations of the octahedral group are distinct from conventional spin representations of the Lorentz group. But one expects that in the continuum limit, the former match onto the latter. Once this extrapolation is achieved, one needs to identify the quantum number J^{PC} of the lattice spectrum. The low-lying states do not lead to ambiguities.

TABLE I: Final continuum-limit glueball mass estimates m_G. When a unique J interpretation for a state cannot be made, the other possibilities are indicated in the second column. States whose interpretation requires further study are indicated by a dagger. In column 3, the first error is the statistical uncertainty from the continuum-limit extrapolation and the second is the estimated uncertainty from the anisotropy. In the final column, the first error comes from the combined uncertainties in $r_0 m_G$, the second from the uncertainty in $r_0^{-1} = 410(20)$ MeV.

J^{PC}	Other J	$r_0 m_G$	m_G (MeV)
0^{++}		4.21 (11)(4)	1730 (50)(80)
2^{++}		5.85 (2)(6)	2400 (25)(120)
0^{-+}		6.33 (7)(6)	2590 (40)(130)
0^{*++}		6.50 (44)(7)†	2670 (180)(130)
1^{+-}		7.18 (4)(7)	2940 (30)(140)
2^{-+}		7.55 (3)(8)	3100 (30)(150)
3^{+-}		8.66 (4)(9)	3550 (40)(170)
0^{*-+}		8.88 (11)(9)	3640 (60)(180)
3^{++}	$6, 7, 9, \ldots$	8.99 (4)(9)	3690 (40)(180)
1^{--}	$3, 5, 7, \ldots$	9.40 (6)(9)	3850 (50)(190)
2^{*-+}	$4, 5, 8, \ldots$	9.50 (4)(9)†	3890 (40)(190)
2^{--}	$3, 5, 7, \ldots$	9.59 (4)(10)	3930 (40)(190)
3^{--}	$6, 7, 9, \ldots$	10.06 (21)(10)	4130 (90)(200)
2^{+-}	$5, 7, 11, \ldots$	10.10 (7)(10)	4140 (50)(200)
0^{+-}	$4, 6, 8, \ldots$	11.57 (12)(12)	4740 (70)(230)

TABLE II: Glueball mass ratios. This ratios are not contaminated by anisotropy errors and are calculated using the empirical fact that correlations between different channels were found negligible. Note that the pseudoscallar glueball is clearly resolved to be heavier than the tensor.

$m(2^{++})/m(0^{++})$	1.39(4)
$m(0^{-+})/m(0^{++})$	1.50(4)
$m(0^{*++})/m(0^{++})$	1.54(11)
$m(1^{+-})/m(0^{++})$	1.70(5)
$m(2^{-+})/m(0^{++})$	1.79(5)
$m(3^{+-})/m(0^{++})$	2.06(6)
$m(0^{*-+})/m(0^{++})$	2.11(6)
$m(0^{-+})\ /m(2^{++})$	1.081(12)

The situation is different for higher states since they can belong to another multiplet with higher excitation not calculated.

Their final results for the glueball spectrum are shown in Fig. 1 and in Table I. In the figure they assume the most likely spin interpretations. The table also contains any alternative spin attributions which cannot be ruled out. Several mass ratios are shown in Table II which can be determined very accurately since they are not contaminated by anisotropy errors. Note that the pseudoscalar glueball is resolved to be heavier than the tensor.

To convert lattice glueball masses into physical units the value of the hadronic scale r_0 must be specified. The estimate used, $r_0^{-1} = 410(20)$ MeV, was obtained by combining Wilson action calculations of a/r_0 with values of the lattice spacing a determined using quenched simulation results of various physical quantities, such as masses of ρ and ϕ mesons, the decay constant f_π, and the $1P - 1S$ splittings in charmonium and bottomonium. A great deal of care should be taken in making direct comparisons with experiments since these values neglect the effects of light quarks and mixings with nearby conventional mesons.

More recently Chen et al.[19] have performed a similar calculation with larger lattices and larger volumes. We present in the Table III a comparison of their results with those of Morningstar and Peardon.[17]

Meyer and Teper investigated also the pure gauge spectrum for (even)$^{++}$ states on a lattice in order to check the linearity of the Pomeron trajectory (see section VII).[18] They reported also masses in other PC sectors. It is instructive to compare their results with the Morningstar and Peardon study.[17] Although in these works absolute masses are expressed with different energy scales (r_0^{-1},[17] and $\sqrt{\sigma}$,[18]), their close values [see Eq. (3)] allow the comparison of their absolute spectra displayed in Fig. 2 (left). Level orderings in both cases are identical but globally Meyer and Teper masses are smaller. Fig. 2 (right) presents mass ratios which are not contaminated by anisotropy

TABLE III: Continuum-limit glueball masses M_G for Chen et al. and for Morningstar and Peardon.

R^{PC}	Possible J^{PC}	$r_0 M_G$ [19]	$r_0 M_G$ [17]
A_1^{++}	0^{++}	4.16(11)	4.21(11)
E^{++}	2^{++}	5.82(5)	5.85(2)
T_2^{++}	2^{++}	5.83(4)	5.85(2)
A_2^{++}	3^{++}	9.00(8)	8.99(4)
T_1^{++}	3^{++}	8.87(8)	8.99(4)
A_1^{-+}	0^{-+}	6.25(6)	6.33(7)
T_1^{+-}	1^{+-}	7.27(4)	7.18(3)
E^{-+}	2^{-+}	7.49(7)	7.55(3)
T_2^{-+}	2^{-+}	7.34(11)	7.55(3)
T_2^{+-}	3^{+-}	8.80(3)	8.66(4)
A_2^{+-}	3^{+-}	8.78(5)	8.66(3)
T_1^{--}	1^{--}	9.34(4)	9.50(4)
E^{--}	2^{--}	9.71(3)	9.59(4)
T_2^{--}	2^{--}	9.83(8)	9.59(4)
A_2^{--}	3^{--}	10.25(4)	10.06(21)
E^{+-}	2^{+-}	10.32(7)	10.10(7)
A_1^{+-}	0^{+-}	11.66(7)	11.57(12)

errors. In this case, errors bars are of the order of the symbols and are not shown.

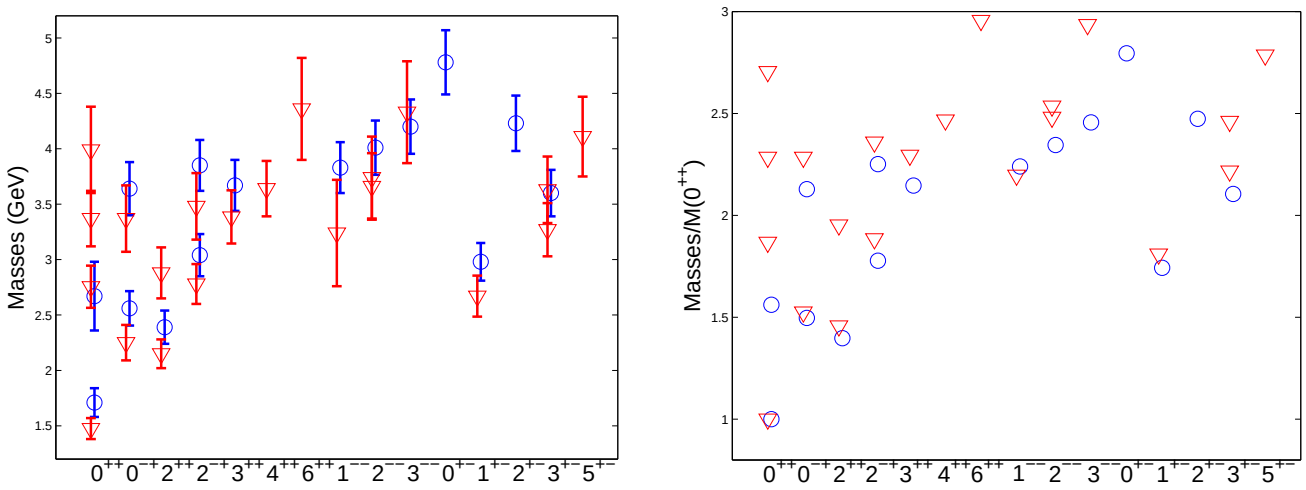

FIG. 2: Comparison between Morningstar and Peardon (circles) and Meyer and Teper (triangles) of the mass spectrum of glueballs in pure $SU_C(3)$ gauge theory. Absolute masses (left) and mass ratios with respect the scalar glueballs (right).

Recently, Meyer updated masses of the scalar and the tensor using his technique.[22] In this latter reference, he used the lattice scale r_0 allowing to compare with the other studies. The new masses are closer the Morningstar and Peardon's ones and read

$$r_0 M_{0^{++}} = 3.958(47), \qquad r_0 M_{2^{++}} = 5.878(77). \tag{6}$$

All lattice calculations are now consistent and shown that, in pure gauge theory, the masses of the lowest states are

$$M_{0^{++}} \sim 1.6 - 1.7 \text{ GeV}, \qquad M_{2^{++}} \sim 2.4 \text{ GeV} . \tag{7}$$

In full QCD interpolating operators for a state with given quantum numbers can also be constructed from quarks and anti-quarks. The pure glue operators might mix with the fermionic operators. If the mixing is very strong, the glueball masses obtained in this way, will have little to do with the glueball masses in the quenched calculation. Several methods have been applied to the interesting scalar sector, $J^{PC} = 0^{++}$, of the physical spectrum.

Weingarten and Lee [23] studied the effect of the effect of quarkonium mixing with the glueball in the lowest 0^{++} state in quenched QCD. The results were expressed as a mixing matrix

$$\begin{pmatrix} m_g & E(s) \\ E(s) & m_\sigma(s) \end{pmatrix} \tag{8}$$

where m_g is the glueball mass, $m_\sigma(s)$ is the mass of the 0^{++} non-singlet $\bar{\psi}\psi$ state, and $E(s)$ is the mixing energy. Weingarten and Lee measured: $m_g = 1648(58)$ MeV, $m_\sigma(s) = 1322(42)$ MeV, and $E(s) = 61(58)$ MeV. The qualitative picture that emerges is that the f_0 (1710) is mostly 0^{++} glueball, and the $f_0(1500)$ is mostly $\bar{s}s$. The mixing energy $E(s)$ has large lattice spacing errors. For example at a lattice spacing of $a^{-1} \sim 1.2$ GeV, the Weingarten and Lee result is $E(s) \sim 0.36$ GeV, while that of McNeile and Michael[24] is $E(s) \sim 0.44$ GeV. The analysis of Weingarten and Lee depends on the 0^{++} states being well defined in quenched QCD. Bardeen et al.[25] have shown that there is a problem with the nonsinglet 0^{++} correlator in quenched QCD. The problem can be understood using quenched chiral perturbation theory. The non-singlet 0^{++} propagator contains an intermediate state of $\eta' - \pi$. The removal of fermion loops in quenched QCD has a big effect on the η' propagator. The result is that a ghost state contributes to the scalar correlator, that makes the expression in Eq. (2) inappropriate to extract masses from the calculation.

A lattice QCD calculation that includes the dynamics of the sea quarks should reproduce the physical spectrum. Some insight into the composition of individual physical states, such as wether the physical particles couple to fermionic operators or pure operators could be studied as an effect of decreasing sea quark mass. Some studies have been performed for $n_f = 2$ QCD [8] and it was found that the mass of the 0^{++} glueball was reduced with respect to the quenched calculation by about 20%. Not so the tensor 2^{++}, whose value remained close to the quenched calculation. The mass of the 0^{++} glueball on the UKQCD data set is degenerate with the mass of two pions.[8] Due to the intricacies of the physical spectrum the lattice spacing used in the unquenched calculations must be reduced before direct contact can be made to phenomenology.

In the real world glueballs have a decay width since they decay into two mesons. Lattice QCD calculations are performed in Euclidean space and this makes the computation of intrinsically complex quantities, as decay widths, complicated.[26] The decay width for the 0^{++} glueball to two pseudoscalars has been calculated to be 108(28) MeV.[27] It is encouraging that it is small compared with its mass, however there is not yet consensus in this result.[28]

III. CONSTITUENT MODELS

Gluon self-coupling in QCD suggests the existence of glueballs. Incontrovertible experimental evidence for their existence remains elusive. A primary reason for this is the difficulty in extracting the properties of glueballs from the QCD lagrangian. We have seen that lattice QCD faces both computational and fundamental problems. We next describe a complementary way to describe glueballs, namely constituent models, which implement in a dynamical way the phenomenological properties of the confining QCD vacuum and the interaction among the gluons.

A. The MIT bag model

Hadrons are physical systems where quarks and gluons are confined in regions smaller than 1 fm. This experimental fact led the physicists of the MIT to develop a bag model of hadrons in QCD.[29] In their picture, quarks and gluons are confined in a bag, usually taken as a static spherical cavity. Confinement is described in the model by a boundary condition and a constant energy density B. The boundary condition makes the color flux vanish at the surface of the bag and it produces a quantization of the energy levels. B gives a constant energy term which stabilizes the bag at a finite size. Energy modes $E_i = x_i/R$ are inversely proportional to the radius of the spherical cavity R. The energy in the cavity under these conditions, with n_i massless constituents of type i, is

$$E = \frac{4\pi B R^3}{3} + \sum_i n_i \frac{x_i}{R}. \tag{9}$$

The bag energy (9) encodes the masses of the states M but also the dynamics of the center-of-mass motion. One solution to this problem is the following: We consider that the bag is an eigenstate of the Hamiltonian $H^2 = \boldsymbol{P}^2 + M^2$. Then we simply take out the quantity

$$\left\langle P^2 \right\rangle = \sum_i n_i \left(\frac{x_i}{R}\right)^2. \tag{10}$$

The mass then reads

$$M^2 = E^2 - \langle P^2 \rangle . \tag{11}$$

In their application to hadrons,[30] the authors considered the bag constant as a free parameters. The minimization of the mass equation leads to a relation between the radius and B. Then the mass equation can be written in terms of only B and by fitting hadronic masses one can determine this parameter.

Jaffe and Johnson were the first to apply this model to glueballs.[6] They found the modes of the gluon field in the cavity corresponding to the solution of the gluon equations of motion subject to the boundary conditions

$$n_\mu G_a^{\mu\nu} = 0, \tag{12}$$

where n_μ is the normal to the bag surface and $G_a^{\mu\nu}$ is the gluon field strength. The two lowest modes are:

$$\text{Transverse Electric} \qquad J^P = 1^+ \qquad x_{\rm TE} = 2.744, \tag{13}$$

$$\text{Transverse Magnetic} \qquad J^P = 1^- \qquad x_{\rm TM} = 4.493. \tag{14}$$

From these one obtains immediatly the masses of the low-lying states: $(\text{TE})^2$, $0^{++}, 2^{++}$, $M = 960$ MeV ; (TE)(TM), $0^{-+}, 2^{-+}$, $M = 1.3$ GeV ; $(\text{TE})^3$, $0^{++}, 1^{+-}, 3^{+-}$, $M = 1.45$ GeV. Some authors pointed out the fact that lowest three-gluon glueballs $0^{++}, 1^{+-}, 3^{+-}$ have the opposite parity to that of the potential model predictions.[31] The parity of the TE mode 1^+ causes this difference. The lattice spectrum seems to support the bag model.

Differently to potential models, constituents in the bag model are not confined by a potential. Particles are almost free inside the bag and the confinement is ensured by the boundary conditions (12). A more elaborated description should lift degeneracies. Carlson *et al.* [32] added to the bag energy (9) a correction ΔE representing the spin splitting induced by one-gluon-exchange interaction. This shift includes tree-level scattering diagrams but also self-energy contributions,

$$\Delta E = \sum_{i \neq j} \Delta E_{ij} + \sum_i \Delta E_i, \tag{15a}$$

$$\Delta E_{ij} = -\frac{\alpha(R)}{R} \langle \boldsymbol{t}_i \cdot \boldsymbol{t}_j (a_{ij} \boldsymbol{S}_i \cdot \boldsymbol{S}_j + b_{ij} T_{ij} + c_{ij} I_{ij}) + d_{ij} \mathcal{P}_{ij} \rangle, \tag{15b}$$

$$\Delta E_i = -\frac{\alpha(R)}{R} \boldsymbol{t}_i^2 e_i, \tag{15c}$$

Here $\boldsymbol{t}_i$ and $\boldsymbol{S}_i$ are the generators of color and spin respectively. $\mathcal{P}$ is the projector onto the color-octet spin-one state. I is the identity operator and $\alpha(R)$ is the running coupling constant,

$$\alpha(R) = \frac{2\pi n}{9} \frac{1}{\ln[1 + 1/(\Lambda R)^n]}. \tag{16}$$

This Ansatz for $\alpha(R)$ simulates the saturation for large R. n is a positive integer parameter. The authors used $n = 2$ and $\Lambda = 0.172$ GeV in their calculations. The coefficients a, b, c, d, e in the relations (15) are given in the reference.

In the original version of the bag model, the bag constant was a free parameter determined from data. Hansson *et al.* proposed a model for the QCD vacuum wich allows B to be calculated given $\alpha(R)$ and $e_{\rm TE}$ (the self-energy of the lowest TE gluon mode).[33] The basic idea is that the vacuum is filled with 0^{++} $(\text{TE})^2$ glueballs which form a negative energy condensate. The expression for B

$$B = \frac{3}{8\pi R_o^3} (-m^2)^{1/2} \tag{17}$$

relates its value to the (negative) mass squared of the scalar glueballs m^2. The excitation of this condensate gives rise to a observable scalar glueballs.[34] Their results are shown in Fig. 3. This figure displays also the glueball spectrum obtained in the bag model of Chanowitz and Sharpe along similar lines.[35] Masses in the bag model are globally lower than in lattice QCD.

In bag models, particles are confined in a spherical bag. This approximation is only valid for totally symmetric $J = 0$ states. Moreover, spherical glueballs are not stable since a vector field can never give rise to a spherically symmetric pressure. Robson pointed out this flaw and developed a toroidal bag model for glueballs.[36] This picture of glueballs is close to the flux tube model of Isgur and Paton.[37]

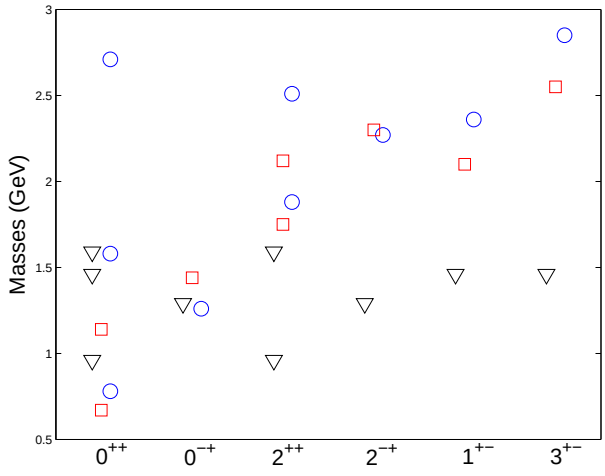

FIG. 3: The mass spectrum of glueballs in bag models: Jaffe and Johnson[6] (triangles), Carlson *et al.*[32] (blue circles) and Chanowitz and Sharpe[35] (squares).

B. Gluon mass

A possible way to handle glueballs is to consider massive quasi-gluons interacting via a QCD inspired dynamics. The gauge bosons are massless at the Lagrangian level but there are hints that they obey massive dispersion relations. The gluons remains massless to all orders in perturbation theory. However, nonperturbative effects, like confinement, and their self-interactions, can be described by a constituent mass. Several definitions exist for this constituent mass.

The so called dynamical mass, is defined by the position of the pole of the dressed gluon propagator. Cornwall arrived to such a dynamical mass by analyzing the gluon Dyson-Schwinger equations in the early 80's.[38] This infinite set of couple equations cannot be solved analytically. One must resort to a truncation scheme. By a clever resummation of Feynman diagrams, Cornwall found a gauge-invariant procedure to deal with these equations. With this technique, a full gluon propagator in quarkless QCD emerges

$$d^{-1}(q^2) = \left(q^2 + m^2(q^2)\right) bg^2 \ln\left[\frac{q^2 + 4m^2(q^2)}{\Lambda^2}\right], \tag{18}$$

with a dynamical mass

$$m^2(q^2) = m^2 \left(\frac{\ln\left[(q^2 + 4m^2)/\Lambda^2\right]}{\ln\left(4m^2/\Lambda^2\right)}\right)^{-12/11}. \tag{19}$$

In Eq. (18), $b = 11N/48\pi^2$ is the first coefficient of the beta function for quarkless QCD and the mass term that appears has finite value at zero momentum. The gluon mass can be related to the gluon condensate $\langle G^a_{\mu\nu} G^{\mu\nu}_a \rangle$ from which the value $m = (500 \pm 200)$ MeV arises.

Bernard proposed a different definition for the gluon mass.[39] Consider the potential energy of a pair of heavy, static sources in the adjoint representation of the color group. As the separation of the adjoint sources (static gluons) is increased, the potential will increase linearly as a string or a flux tube is formed between them. The energy stored in the string will at some point be large enough to pop up a pair of dynamical gluons out of the vacuum. The effective gluon mass is defined as half of the energy stored in the flux tube at this point. Monte-Carlo simulations of this phenomenon show a effective gluon mass in the range 500-800 MeV.

The effective gluon mass was also investigated in the bag model.[40] Even though the gluon is massless in the bag model, a net energy of 740 ± 100 MeV is required to produce a gluon due to confinement.

All these arguments support the use of an effective gluon mass to describe the dynamics of QCD. It is therefore possible to envisage an approach to bound states made of *constituent* massive gluons. Since two-gluon glueballs have always a positive conjugation charge, a study of the full spectrum must include also three-gluon glueballs.

C. Two-gluon glueballs

One of the pioneering works on two-gluon glueballs was the study by Cornwall and Soni.[41] The large value of the effective gluon mass led them to propose a nonrelativistic approach to gluonium. They used a confining potential which saturates at large distances constrained by Bernard's results[39]

$$V_C(r) = 2m\left(1 - e^{-r/r_s}\right). \tag{20}$$

This screened potential led to a spectrum with relatively low glueball masses. The scalar and tensor glueballs had masses around ~ 1.3 and ~ 1.6 GeV, respectively. They used for the string tension twice the value commonly used for mesons, a decision which they justified by arguing that a gluon acts as a $q\bar{q}$ pair. The Coulomb and spin-dependent interactions at short-range were derived from a nonrelativistic expansion of the Feynman graphs for two-gluon scattering. They considered massive exchanged gluons (with the same mass as the constituent one) to keep the gauge invariance of the amplitudes to the given order. This one-gluon exchange (OGE) potential involves Yukawa, spin-orbit, spin-spin and tensor forces,

$$\begin{aligned} V_{\rm oge}(\boldsymbol{r}) = &-\frac{\lambda e^{-mr}}{r}\left(\frac{2s-7m^2}{6m^2}+\frac{1}{3}\boldsymbol{S}^2\right)+\frac{\pi\lambda\delta(\boldsymbol{r})}{3m^2}\left(\frac{4m^2-2s}{m^2}+\frac{5}{2}\boldsymbol{S}^2\right)\\ &-\frac{3\lambda}{2m^2}\boldsymbol{L}\cdot\boldsymbol{S}\frac{1}{r}\frac{\partial}{\partial r}\frac{e^{-mr}}{r}+\frac{\lambda}{2m^2}\left[(\boldsymbol{S}\cdot\boldsymbol{\nabla})^2-\frac{1}{3}\boldsymbol{S}^2\boldsymbol{\nabla}^2\right]\frac{e^{-mr}}{r}. \end{aligned} \tag{21}$$

s is the glueball mass squared, which we can set to $s = 4m^2$ in a first approximation, and $\lambda = 3\alpha_s$ is the strong coupling constant.

Cornwall and Soni presented results for states with quantum numbers $L = 0$, $J^{PC} = 0^{++}, 2^{++}$, and $L = 1$, $J^{PC} = 1^{-+}, 2^{-+}$. Despite the fact that the gluons acquire a mass they remain transverse. For transverse particles the $J = 1$ states are forbidden as a consequence of Yang's theorem,[42] *i.e.*, a gluon in a massless representation has only two projections for its spin and therefore two transverse gluons cannot bind into a $J = 1$ state. Thus we must incorporate this feature into the above formalism.

When dealing with massless representations, the conventional $\boldsymbol{J} = \boldsymbol{L} + \boldsymbol{S}$ decomposition is not useful anymore. The formalism to treat two-body relativistic scattering developed by Jacob and Wick[43] allows also the description of representations with only transverse gluons. We sketch its main features and apply this formalism to the study of the two-gluon glueball.

The Jacob and Wick formalism is based on states, $|J, M; \lambda_1, \lambda_2\rangle$, which are eigenstates of $\boldsymbol{J}^2$ and J_z and where λ_1 and λ_2 represent the two allowed spin projections. In the case under consideration, the projections can only be maximal, *i.e.* $\pm s$ for a particle with helicity-s . The angular part of these states are related with the conventional basis states by means of Clebsch-Gordan coefficients:

$$|J, M; \lambda_1, \lambda_2\rangle = \sum_{L,S}\left[\frac{2L+1}{2J+1}\right]^{1/2}\langle LS0\Lambda|\, J\Lambda\,\rangle\,\langle s_1 s_2\lambda_1(-\lambda_2)|\, S\Lambda\,\rangle\,\left|^{2S+1}L_J\right\rangle, \tag{22}$$

with $\Lambda = \lambda_1 - \lambda_2$. The radial part (depending on J) is determined variationally with the Hamiltonian. The states are not eigenstates of parity. For a two-gluon state, $s_1 = s_2 = 1$, it holds

$$\hat{P}\,|J, M; \lambda_1, \lambda_2\rangle = (-1)^J\,|J, M; -\lambda_1, -\lambda_2\rangle. \tag{23}$$

The key point is that physical states must not only be eigenstates of the total angular momentum operator but they must also be eigenstates of parity. Such a requirement is fulfilled by the following linear combinations

$$\left|H_\pm; J^P; \lambda_1, \lambda_2\right\rangle = \frac{1}{\sqrt{2}}\left\{\,|J, M; \lambda_1, \lambda_2\rangle \pm |J, M; -\lambda_1, -\lambda_2\rangle\right\}, \tag{24}$$

for which $\mathsf{P}\left|H_\pm; J^P; \lambda_1, \lambda_2\right\rangle = P\left|H_\pm; J^P; \lambda_1, \lambda_2\right\rangle$, with $P = \pm(-1)^J$. In the latter, the $\left|H_\pm; J^P; \lambda_1, \lambda_2\right\rangle$ states will be referred as helicity states. When the two particles are identical, the wave function should be an eigenvector of the permutation operator P_{12}. The basic state (24) are eigenstate of the permutation in the case of massless particles since $\lambda_1 = \pm\lambda_2$ and[43]

$$\mathrm{P}_{12}\,|J, M; \lambda_1, \lambda_2\rangle = (-1)^J\,|J, M; \lambda_2, \lambda_1\rangle. \tag{25}$$

A system of two gluons has to be totaly symmetric and this constraint leads to selection rules on the spin and the parity. Indeed, for singlet states (defined by $\lambda_1 = \lambda_2 = \lambda$), we have

$$\mathrm{P}_{12} \left|H_\pm; J^P; \lambda, \lambda\right\rangle = (-1)^J \left|H_\pm; J^P; \lambda, \lambda\right\rangle, \tag{26}$$

leading to the families with the even spin and positive or negative parity . The minimum spin in this case is $J = 0$. For the doublet (defined by $\lambda_1 = -\lambda_2 = \lambda$), the minimum spin is $J = 2$ and we have

$$\mathrm{P}_{12} \left|H_\pm; J^P; \lambda, -\lambda\right\rangle = \pm(-1)^J \left|H_\pm; J^P; \lambda, -\lambda\right\rangle. \tag{27}$$

This time we can have odd spin (the lowest is 3^+) but also even spin with positive parity. We thus observe the emergence of selection rules according to the value of J and P.

The results for states of two transverse gluons are formally identical to the case of states made of two photons, *i.e.*, Yang's theorem.[42] The total color wave function is assumed to be a singlet, which is totally symmetric, and does not explicitly appear in the computations. Taking into account the Bose symmetry, one finds that there are four allowed helicity states, namely

$$\left|S_\pm; J^P\right\rangle = \left|H_\pm; J^P\right\rangle_{\lambda_2=\lambda_1}, \tag{28a}$$

$$\left|D_\pm; J^P\right\rangle = \left|H_\pm; J^P\right\rangle_{\lambda_2=-\lambda_1}. \tag{28b}$$

The selection rules impose restrictions to the possible values of the total angular momentum and parity of these four types of states. It can be checked that one can only obtain the following states

$$\left|S_+; (2k)^+\right\rangle, \quad \left|S_-; (2k)^-\right\rangle, \quad \left|D_+; (2k+2)^+\right\rangle, \quad \left|D_-; (2k+3)^+\right\rangle, \quad k \in \mathbb{N}. \tag{29}$$

The S- and D-labels stand for helicity-singlet and -doublet respectively. We recognized in Eq. (29) the four families predicted by Yang.[42]

It should be noted that a state made of two gluons in a color singlet state has always positive charge conjugation ($C = +1$). More explicitly, the states in Eq. (29) give rise to the following glueball states

$$\left|S_+ \,;\, (2k)^+ \right\rangle \;\Rightarrow\; 0^{++}, 2^{++}, 4^{++}, \ldots \tag{30a}$$

$$\left|S_- \,;\, (2k)^- \right\rangle \;\Rightarrow\; 0^{-+}, 2^{-+}, 4^{-+}, \ldots \tag{30b}$$

$$\left|D_+; (2k+2)^+\right\rangle \;\Rightarrow\; 2^{++}, 4^{++}, \ldots \tag{30c}$$

$$\left|D_-; (2k+3)^+\right\rangle \;\Rightarrow\; 3^{++}, 5^{++}, \ldots \tag{30d}$$

It is readily observed that only the $|S_\pm; (2k)^+\rangle$ states can lead to $J = 0$, while the $|D_\pm\rangle$ states always have $J \geq 2$ (since $J > |\lambda_1 - \lambda_2|$). Obviously, a consequence of Yang's theorem is that no $J = 1$ states are present. Only the $|D_-\rangle$ states can generate an odd-J, but J is at least 3 in this case.

Lattice QCD confirms the absence of the 1^{-+} and 1^{++} states, at least below 4 GeV. It is worth mentioning that glueball states with even-J and positive parity can be built either from the helicity-singlet or from the helicity-doublet states. The important result is that the gluons remain transverse and therefore the helicity formalism exactly reproduces the J^{PC} content for glueballs which is observed in lattice QCD, without the extra states which are usually present in potential models.

The helicity formalism was applied for the first time by Barnes.[44] It has several advantages not shared by the more conventional nonrelativistic LS-basis. It avoids spurious states forbidden by the coupling of two transverse gluons but also reproduces the lattice QCD hierarchy, *i.e.*

$$0^{\pm+}, 2^{++}, 2^{\pm+}, 3^{++}, 4^{++}, 4^{\pm+}, 5^{++}, 6^{++}. \tag{31}$$

Within this approach, a given J^{PC} state can be expressed as a linear combination of (L, S) states thanks to Eq. (22). The complete expressions for these decompositions can be found in Mathieu *et al.*[45] We give here the angular dependence of the ground states of Eq. (30):

$$\left|S_+; (0)^+\right\rangle = \sqrt{\frac{2}{3}} \left|{}^1S_0\right\rangle + \sqrt{\frac{1}{3}} \left|{}^5D_0\right\rangle, \tag{32a}$$

$$\left|S_-; (0)^-\right\rangle = \left|{}^3P_0\right\rangle, \tag{32b}$$

$$\left|D_+; (2)^+\right\rangle = \sqrt{\frac{2}{5}} \left|{}^5S_2\right\rangle + \sqrt{\frac{4}{7}} \left|{}^5D_2\right\rangle + \sqrt{\frac{1}{7}} \left|{}^5G_2\right\rangle, \tag{32c}$$

$$\left|D_-; (3)^+\right\rangle = \sqrt{\frac{5}{7}} \left|{}^5D_3\right\rangle + \sqrt{\frac{2}{7}} \left|{}^5G_3\right\rangle. \tag{32d}$$

These decompositions are essential for computing the matrix elements of relativistic operators (spin-spin, spin-orbit and tensor). Let us note that the matrix elements of these operators are equal for $|S_+;(2k)^+\rangle$ and $|S_-;(2k)^-\rangle$.[45]

Even though in this approach the singlet states $J^P = (2k^+, 2k^-)$ are degenerate, with a Cornell-type (linear + Coulomb) potential, a nonrelativistic kinetic energy, which incorporates an *ad hoc* gluon mass m, and using the helicity formalism, Barnes was able to reproduce the qualitative feature of the pure gauge sector finding $M(0^{\pm+}) = 4.36\,m$. The higher mass ratios were not in perfect agreement with modern lattice results, implying the need for modifications.

We emphasize that considering transverse gluons is essential for finding the correct hierarchy. However, transverse particles are generally massless and even if nonperturbative effects are able to give a mass to the gluon, one may wonder if a nonrelativistic kinetic energy $\boldsymbol{p}^2/2m$ is appropriate. Indeed, the nonrelativistic kinetic energy is just the limit of the more general Dirac operator $\sqrt{\boldsymbol{p}^2 + m^2}$. This semi-relativistic energy is also valid for massless particles such as gluons.

Brau and Semay compared different models for glueballs.[46] Models with a nonrelativistic kinetic energy were not able to reproduce correctly the lattice gauge spectrum for realistic values of the parameters. They concluded that a semi-relativistic Hamiltonian, *i.e.* $2\sqrt{\boldsymbol{p}^2} + V(r)$, is an essential ingredient to handle glue states. Nevertheless, all models analyzed used an LS-basis and were plagued with unwanted states. Moreover, they had to include the short-range potential Eq. (21) to lift some degeneracies between the states. This is not the case if we implement transverse gluons by means of the Jacob and Wick formalism, then automatically the degeneracies are lifted.

This improvement was carried out in a work based on the Coulomb gauge Hamiltonian where a relativistic kinetic energy was used.[47] In this model, gluons are linked by an adjoint string. The adjoint string tension $\sigma_A = (9/4)\sigma$ is expressed in terms of the well-known fundamental string tension for mesons σ through the Casimir scaling hypothesis supported by lattice calculations.[48] Using typical values for the parameters, $\sigma = 0.18$ GeV^2 for the fundamental string tension (extracted from mesons Regge trajectory) and $\alpha_S = 0.4$ for the strong coupling, this model encodes the essential features of glueballs.

The spectrum of the Coulomb gauge Hamiltonian was in good agreement with lattice QCD. Moreover, the singlet 2^{-+} and 2^{++} are degenerate as in the Barnes' model, a characteristic of the helicity formalism. The authors found a difference between the scalar and pseudoscalar glueballs. This splitting, about 250 MeV was nevertheless not as strong as in lattice QCD (800 MeV).

Recently, this problem was revisited keeping the basic ingredients needed for obtaining an acceptable pure gauge spectrum compatible with lattice results, *i.e.* semi-relativistic energy and the helicity formalism for two transverse gluons.[45] A simple Cornell potential was used but an instanton induced force was added and with it the splitting between the scalar and pseudoscalar glueballs was reproduced. There are arguments favoring an attractive (repulsive) interaction induced by instantons in the scalar (pseudoscalar) channel of glueballs.[49]

In all the constituent models for glueballs, the confining interaction follows from phenomenological considerations (breakable strings or linear potentials). But it is also possible to derive an effective Hamiltonian for bound states from the QCD Lagrangian. Kaidalov and Simonov used the field correlator method to extract a relativistic Hamiltonian which describes an adjoint string with gluons at its ends.[50] The introduction of auxiliary fields (or einbein field) μ and ν leads to

$$H_0 = \frac{p_r^2}{\mu} + \mu + \frac{L(L+1)}{r^2\left[\mu + \int_0^1 (\beta - \frac{1}{2})^2 \nu d\beta\right]} + \int_0^1 \frac{\sigma_A^2 d\beta}{2\nu} r^2 + \frac{1}{2}\int_0^1 \nu d\beta. \tag{33}$$

In Eq. (33), μ is introduced to get rid of the square root and $\langle\mu\rangle = \langle\sqrt{\boldsymbol{p}^2}\rangle$ represents the effective gluon energy. $\langle\nu\rangle$ is the energy stored in the rotating string. The einbeins are eliminated using the equations of motion, $\delta_\mu H_0 = \delta_\nu H_0 = 0$. For $L = 0$, we find $\nu = \sigma_A r$, and the replacement of the auxiliary field leads to

$$H_0 = 2\sqrt{\boldsymbol{p}^2} + \sigma_A r. \tag{34}$$

For $L \neq 0$ it is not possible to eliminate ν analytically and the optimization $\delta_\nu H_0 = 0$ should be done numerically.

In this approach, gluons are massless but gain an effective mass $\mu_0 = \langle\mu\rangle \sim 0.5$-$1$ GeV. The expectation value is taken on an eigenstate of H_0 therefore μ_0 is state-dependent. The spin splitting operators are corrections of order μ_0^{-2} and are computed perturbatively. These corrections contain the conventional structure arising from the one-gluon-exchange and, in addition, a spin-orbit term coming from the Thomas precession,

$$\begin{aligned}\Delta H = &-\frac{\lambda}{r}+\frac{\lambda}{r^3}\frac{\boldsymbol{L}\cdot\boldsymbol{S}}{\mu_0^2}+\frac{8\pi\lambda}{3\mu_0^2}\delta(\boldsymbol{r})\boldsymbol{S}_1\cdot\boldsymbol{S}_2\\ &+\frac{\lambda}{r^3\mu_0^2}\left(3(\boldsymbol{S}_1\cdot\hat{\boldsymbol{r}})(\boldsymbol{S}_2\cdot\hat{\boldsymbol{r}})-\boldsymbol{S}_1\cdot\boldsymbol{S}_2\right)\\ &-\frac{\sigma_A}{r}\frac{\boldsymbol{L}\cdot\boldsymbol{S}}{2\mu_0^2}\end{aligned} \tag{35}$$

with $\lambda = 3\alpha_s$.

The numerical results for the two-gluon glueballs in all the models discussed are displayed in Table IV and Fig. 4

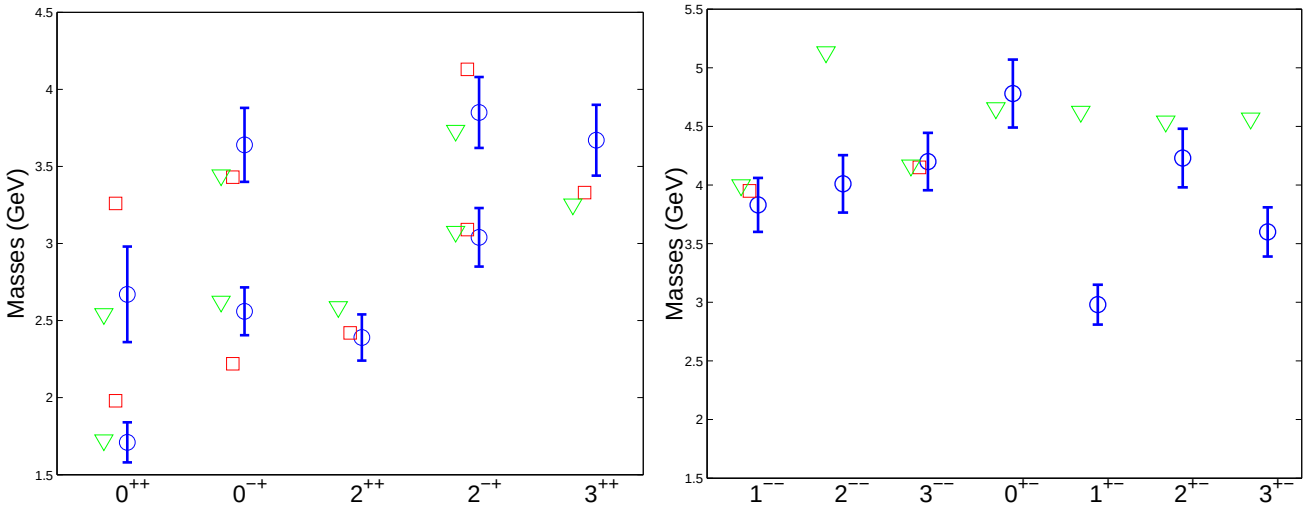

FIG. 4: Comparison between lattice results 17 (circles) and two-gluon glueballs (left) from Ref. 47 (squares) and Ref. 45 (triangles) and three-gluon glueballs (right) from Ref. 55 (squares) and Ref. 57 (triangles).

TABLE IV: Two-gluon glueballs spectra in different models. In brackets, the ratios with respect to the scalar glueball. Masses are in GeV.

J^{PC}	ref. [44]	ref. [47]	ref. [45]	ref. [51]	ref. [17, 19]	ref. [18]
0^{++}	(1.00)	1.98(1.00)	1.72(1.00)	1.41(1.00)	1.71(1.00)	1.48(1.00)
	(1.40)	3.26(1.65)	2.54(1.48)	2.41(1.71)	2.67(1.56)	2.76(1.89)
0^{-+}	(1.00)	2.22(1.12)	2.62(1.52)	2.28(1.62)	2.56(1.50)	2.25(1.54)
	(1.40)	3.43(1.73)	3.44(2.00)	3.35(2.38)	3.64(2.13)	3.37(2.31)
2^{++}	(1.16)	2.42(1.22)	2.59(1.51)	2.30(1.63)	2.39(1.40)	2.15(1.47)
	(1.35)	3.11(1.57)	3.08(1.79)	3.32(2.35)		2.88(1.97)
2^{-+}	(1.35)	3.09(1.56)	3.08(1.79)	2.70(1.91)	3.04(1.78)	2.78(1.90)
	(1.68)	4.13(2.09)	3.73(2.17)	3.73(2.65)	3.89(2.27)	3.48(2.38)
3^{++}	(1.42)	3.33(1.68)	3.25(1.89)		3.67(2.15)	3.39(2.32)
4^{++}	(1.63)	3.99(2.02)	3.77(2.19)			3.64(2.49)
	(1.71)	4.28(2.16)	3.96(2.30)			
4^{-+}	(1.71)	4.27(2.16)	3.96(2.30)			
5^{++}			4.21(2.45)			
6^{++}			4.60(2.67)			4.36(2.98)

The low-lying positive C-parity glueball states, seem to favor a constituent picture with two gluons interacting via a linear potential, *i.e.* linked by a string. A relativistic approach with two transverse gluons leads to a spectrum in good agreement with the lattice hierarchy.

This stringy picture leads to a Regge trajectory

$$J \sim \frac{1}{2\pi\sigma}M^2, \tag{36}$$

well-known in the meson sector. The experimental slope for mesons $1/(2\pi\sigma) \approx 0.9$ GeV^{-2} corresponds to the typical value for a fundamental string tension $\sigma \approx 0.18$ GeV^2. When we extend this picture to glueballs, the slope rises to 0.4 GeV^{-2} if the Casimir scaling hypothesis is used. If one argues that even spin positive C-parity glueballs lie on the pomeron trajectory, a problem arises. Indeed, the experimental soft pomeron slope is $\alpha' \approx 0.25$ GeV^{-2}. Since the pomeron trajectory carries physical particles, a first solution is that glueballs probably mix with quark states. Let us note before finishing this discussion that to describe negative C-parity states in constituent models one needs at least three gluons.

A very different approach to the interpretation of the spectrum is in terms of a closed flux tubes. This picture was introduced by Isgur and Paton.[37] This model is composed by a closed loop of fundamental flux with no constituents gluons at all. Such a loop has phononic and orbital degrees of excitation. These two modes lead to two Regge behaviors at large spin,

$$\text{phononic}: \; J \sim \frac{1}{8\pi\sigma} M^2, \qquad\qquad \text{orbital}: \; J \sim \frac{3\sqrt{3}}{32\pi\sigma} M^2. \tag{37}$$

In either case one obtains a slope 0.2-0.3 GeV^{-2} which is in the right range for the pomeron [see Eq. (62)].[18] Another interesting feature of the closed flux tube model is the appearance of low-lying odd spin $PC = +-$ states in the spectrum. In their original paper, Isgur and Paton discussed masses for some low-lying pure glue states (see Fig. V).[37]. These authors argued that the true values of their parameters were not known and they simply chose them to fit expected results. The splittings are not sensitive to their choice of parameters but their absolute values are.

TABLE V: Low lying glueball states in the flux tube model.

J^{PC}	Mass (GeV)
0^{++}	1.52
1^{+-}	2.25
0^{++}	2.75
$0^{++}, 0^{+-}, 0^{-+}, 0^{--}$	2.79
2^{++}	2.84
$2^{++}, 2^{++}, 2^{++}, 2^{++}$	2.84
1^{+-}	3.25
3^{+-}	3.35

D. Three-gluon glueballs

A complete investigation of the glueball spectrum in constituent models has to include three-gluon glueballs. Indeed, in this approach negative C-parity glueballs involve at least three constituents. There are two color wave functions, totally symmetric or totally antisymmetric, coupling three adjoint representations into a singlet. They do not mix and we are only interested in the symmetric one, $d_{abc} A^a_\mu A^b_\nu A^c_\rho$, namely the $C = -$ states.

Soni with Hou extended his paper with Cornwall to three massive gluons.[54] Their potential is a generalization of the previous one,

$$V_{ggg} = \sum_{i<j} \frac{1}{2} V_C(r_{ij}) + V^{oge}_{ggg}(r_{ij}), \tag{38}$$

with V_C the confining potential of the breakable string of Eq. (20). A factor one-half is added because one needs to remove three (and not six) gluons from the vacuum to screen the three gluons that are originally there in the glueball. The short-range potential is not the OGE potential Eq. (21) with a different color factor, because one should also take into account the annihilation diagram not present in two-gluon glueballs, but it involves the same structures (spin-spin, tensor and spin-orbit interactions). The nonrelativistic kinetic energy and the screened confining potential lead to a spectrum which is too low. The low-lying states are nearly degenerate with a mass 4.8 times the constituent mass m of the gluons. By low-lying, the authors mean that every pair of particles is an S-wave. Symmetry considerations on the total wave function imply that the low-lying states are the $0^{-+}, 1^{--}, 3^{--}$.

The 3^{--} is the lowest maximum spin state. One often argues that such states with maximal spin lie on the odderon trajectory, the counterpart to the pomeron trajectory in hadron-hadron scattering at high energy. The linearity of the odderon trajectory was checked using a Coulomb gauge Hamiltonian.[55] Their masses for the $1^{--}, 3^{--}, 5^{--}, 7^{--}$ are shown in Table VI.

TABLE VI: Odderon quantum numbers and masses in MeV.

J^{PC}	Conf.	σ (GeV^2)	1^{--}	3^{--}	5^{--}	7^{--}
S			1	3	3	3
L			0	0	2	4
Llanes-Estrada[55]	Δ	0.18	3950	4150	5050	5900
Simonov[50]	Δ	0.238	3490	4030		
Simonov[51]	Δ	0.18	3020	3490	4180	4960
	Y	0.18	3320	3830	4590	5250
Mathieu[56, 57]	Y	0.21	3999	4167	5263	
Lattice[19]		0.1939	3830	4200		
Lattice[18]		0.1939	3100	4150		

In their Coulomb gauge approach to three-gluon glueballs, these authors chose a spin-independent potential which is a sum of two-body Cornell ones and a Δ-shape for confinement. Another Ansatz for the confinement, the Y-shape, is sometimes preferred. The Y-shape is the generalization of confinement in baryons where every quark provides a flux tube. These flux tubes coming from gluons meet in a point where the total energy (or the length since the energy density is constant) is minimal. It is worth mentioning that, under the Casimir scaling hypothesis, a simple application of the triangular inequalities shows that the Δ-shape is energetically more favorable than the Y-shape.[52] This demonstration was recently confirmed by a lattice study of the three-gluon potential.[53]

Kaidalov and Simonov investigated both Ansätze for confinement with a nonrelativistic Hamiltonian[51]

$$H_{ggg} = \frac{\boldsymbol{p}_1^2 + \boldsymbol{p}_2^2 + \boldsymbol{p}_3^3}{2\mu} + \frac{3\mu}{2} + V_{\Delta,Y}(\boldsymbol{r}_1, \boldsymbol{r}_2, \boldsymbol{r}_3), \tag{39}$$

with

$$V_\Delta(\boldsymbol{r}_1, \boldsymbol{r}_2, \boldsymbol{r}_3) = \sigma \sum_{i<j} |\boldsymbol{r}_i - \boldsymbol{r}_j|, \qquad V_Y(\boldsymbol{r}_1, \boldsymbol{r}_2, \boldsymbol{r}_3) = \frac{9}{4}\sigma \sum_{i=1}^{3} |\boldsymbol{r}_i - \boldsymbol{R}_Y|. \tag{40}$$

They found the eigenvalues of this operators by using the hyperspherical formalism. The spin-average masses of this Hamiltonian for the odderon states $(\text{odd})^{--}$ are displayed in Table VI. Clearly, the Y-shape potential leads to a higher spectrum than the Δ-shape one.

TABLE VII: Glueball spectrum in the $PC = +-$ sector.

J^{PC}	Lattice[19]	Mathieu[57]	Simonov[51]
0^{+-}	4780	4656	4090
1^{+-}	2980	4626	4090
2^{+-}	4230	4542	4090
3^{+-}	3600	4568	4090
5^{+-}	4110 [18]	5317	

As we saw in the case of two-gluon glueballs, a nonrelativistic description of such states is not appropriate. However, in the negative C-parity sector, the lack of lattice results for high spin states does no allow us to draw any definitive conclusions. Also, the Regge trajectory of the odderon is not well understood yet. New theoretical and experimental research on these topics would be helpful for understanding these glueballs.

On the other hand, lattice QCD exhibits an interesting spectrum in the $PC = +-$ sector. There is nearly 2 GeV between the lowest 1^{+-} state and the highest 0^{+-}. According to the LS decomposition in constituent models, all these states $(0^{+-}, 1^{+-}, 2^{+-}, 3^{+-})$ should be $L = 1$ and degenerate. This feature appears clearly in Simonov and Kaidalov's paper.[51]

Using a generalization of the Hamiltonian Eq. (39) but with a semi-relativistic kinetic energy, Mathieu *et. al* found also a degeneracy between the J^{+-} states in disagreement with the lattice results.[57] Their Hamiltonian involves a Y-junction at the center of mass for the confinement and an OGE potential for the short-range part

$$H = \sum_{i=1}^{3} \sqrt{\boldsymbol{p}_i^2} + a \sum_{i=1}^{3} |\boldsymbol{r}_i - \boldsymbol{R}_0| + V_{\rm OGE}. \tag{41}$$

Their study is an extension of a first one where only $L = 0$ states were considered.[56] The parameters for this three-gluon glueball model were fitted on the two-gluon glueballs of a previous work.[46] Previously, the 2^{--} had been computed with the wrong wave function.[55] In this study, the right 2^{--} state was obtained. It was noted that this result disagrees with that of lattice QCD.[56] In a model with longitudinal gluons, the 2^{--} cannot lie between the 1^{--} and the 3^{--} as lattice calculations have shown (cf. Fig 4). This was a hint that a description with the nonrelativistic decomposition $\boldsymbol{J} = \boldsymbol{L} + \boldsymbol{S}$ should be inadequate to handle the pure gauge spectrum. In the $PC = +-$ sector, all states within this approach lie in the same range and they contradict the lattice results. Hence, we conclude that a description of many-gluon states with a LS-basis is not appropriate. A solution could be to implement the helicity formalism for three particle states for three transverse gluons. One hopes that then it would be possible to reproduce the correct hierarchy. Indeed, the lowest states with three longitudinal gluons are the 1^{--} and 3^{--} while in lattice QCD the lowest negative C-parity are the 1^{+-} and 3^{+-}.

E. AdS/QCD

An alternative approach to strong interactions is based on the idea that they have a description in terms of strings. A remarkable step in this direction was given by Maldacena proposing the equivalence between conformal fields and string theory in anti-de Sitter spacetime (AdS/CFT correspondence).[58] In particular glueball operators of the conformal gauge theory defined on the AdS boundary are in correspondence with the string dilaton field. The description of the strong interactions based on this correspondence requires the breaking of conformal invariance, which can be done in different ways. The spectrum of the glueball has been calculated in two of these models for breaking. The first introduces a Schwarzschild black hole in AdS to break scale invariance.[59] The corresponding supergravity equations do not admit closed form solutions and the spectrum has been calculated using approximate methods (see Table VIII).[60, 61] The second possibility is to imitate the Randall-Sundrum model by considering two slices of AdS sticked together assuming that there is a bulk/boundary correspondence between the glueballs and the dilaton.[62] Imposing boundary conditions the string dilaton acquires discrete modes and these modes become the spectrum of glueballs (see Table VIII).

Let us for the purposes of illustration, describe the analysis of the complete glueball spectrum calculation for the AdS^7 black hole supergravity dual of QCD_4 in strong coupling limit: $g^2N \to \infty$.[61] Despite the expected limitations of a leading order strong coupling approximation, the pattern of spins, parities and mass inequalities bare a striking resemblance to the known QCD_4 glueball spectrum as determined by lattice simulations at weak coupling.

To approach QCD_4 one begins with M theory on $\mathbf{AdS^7} \times \mathbf{S^4}$. One compactifies the "eleventh" dimension (on a circle of radius R_1) to reduce the theory to type IIA string theory and then following the suggestion of Witten raise the "temperature", β^{-1}, with a second compact radius R_2 in a direction τ, with $\beta = 2\pi R_2$. On the second "thermal" circle, the fermionic modes have anti-periodic boundary conditions breaking conformal and all SUSY symmetries. This lifts the fermionic masses and also the scalar masses, through quantum corrections. The 't Hooft coupling is $g^2N = 2\pi g_s N l_s/R_2$, in terms of the closed string coupling, g_s and the string length, l_s . Therefore, in the scaling limit, $g^2N \to 0$, if all goes as conjectured, there should be a fixed point mapping type IIA string theory onto $SU(N)$ pure Yang-Mills theory.

One considers the strong coupling limit at large N, where the string theory becomes classical gravity in the AdS^7 black hole metric,

$$ds^2 = (r^2 - \frac{1}{r^4})d\tau^2 + r^2 \sum_{i=1,2,3,4,11} dx_i^2 + (r^2 - \frac{1}{r^4})^{-1} dr^2 + \frac{1}{4} d\Omega_4^2 \,, \tag{42}$$

with radius of curvature, $R_{AdS}^3 = 8\pi g_s N l_s^3$. The dimensionful parameters have been removed in the metric by a normalization setting $R_{AdS} = 1$ and $\beta = 2\pi/3$.

TABLE VIII: Masses of glueball states J^{PC} with even J expressed in GeV, estimated using the sliced $AdS_5 \times S^5$ space with Dirichlet (Neumann) boundary conditions.[63] The mass of 0^{++} is an input from lattice results.[17,64]

Dirichlet glueballs	lightest state	1^{st} excited state	2^{nd} excited state
0^{++}	1.63	2.67	3.69
2^{++}	2.41	3.51	4.56
4^{++}	3.15	4.31	5.40
6^{++}	3.88	5.85	6.21
8^{++}	4.59	5.85	7.00
10^{++}	5.30	6.60	7.77

Neumann glueballs	lightest state	1^{st} excited state	2^{nd} excited state
0^{++}	1.63	2.98	4.33
2^{++}	2.54	4.06	5.47
4^{++}	3.45	5.09	6.56
6^{++}	4.34	6.09	7.62
8^{++}	5.23	7.08	8.66
10^{++}	6.12	8.05	9.68

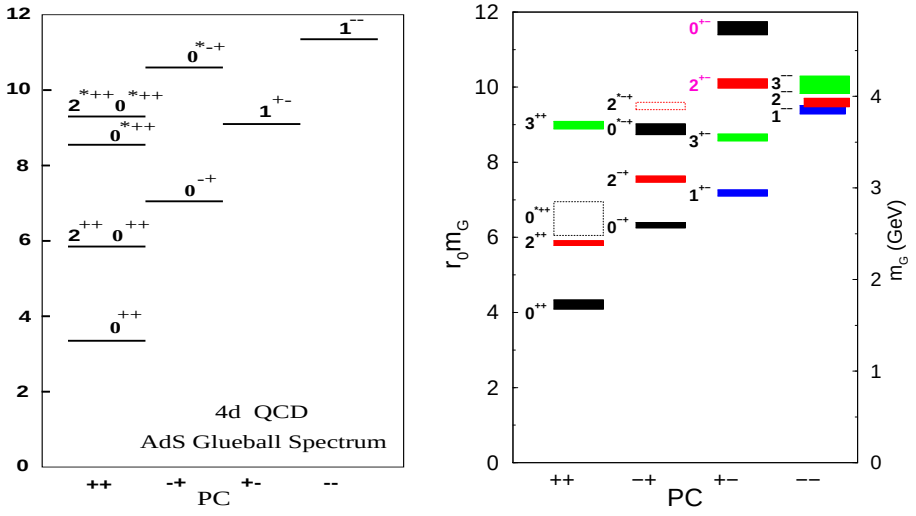

FIG. 5: The AdS glueball spectrum[61] for QCD_4 in strong coupling (left) compared with the lattice spectrum[17] for pure SU(3) QCD (right). The AdS cut-off scale is adjusted to set the lowest 2^{++} tensor state to the lattice results in units of the hadronic scale $1/r_0 = 410$ Mev.

The strong coupling glueball calculation consists of finding the normal modes for the bosonic components of the supergraviton multiplet in the $\mathbf{AdS^7 \times S^4}$ black hole background. We are only interested in excitations that lie in the superselection sector for QCD_4. Imposing this restriction and exploiting symmetries of the background metric reduce the problem to six independent wave equations which have to be solved with the appropriate boundary conditions.

There is a rather remarkable correspondence of the overall mass and spin structure between strong coupling glueball spectrum and the lattice results at weak coupling for QCD_4, see Fig. 5. Apparently the spin structure of type IIA supergravity does resemble the low mass glueball spin splitting. The correspondence is sufficient to suggest that the Maldacena duality conjecture may well be correct and that further efforts to go beyond strong coupling are worthy of sustained effort.

The basic idea behind the AdS/CFT correspondence is that the low mass glueball spectrum can be qualitatively understood in terms of local gluon interpolating operators of minimal dimension an idea which is not new.[5, 65]

These operators are in rough correspondence with all the low mass glueballs states, as computed in a constituent gluon or bag models discussed previously. Thus the AdS/QCD if valid would justify the behavior of the gluon as a constituent. Let us note, however, that in constituent models, confinement is ensured by the potential and in the bag model and AdS/QCD, by a boundary conditions.

IV. GLUEBALLS AND QCD SUM RULES

The QCD sum rule (SR) approach is one of the most widely used methods to obtain the information about glueball properties.[66, 67, 68, 69] It is based on the operator product expansion (OPE) of the correlator of two glueball interpolating currents J_G

$$\Pi(Q^2) = i \int d^4x \; e^{iq\cdot x} \langle 0|T J_G(x) J_G(0)|0\rangle \tag{43}$$

in the deeply-Euclidean domain $Q^2 = -q^2 \gg \Lambda^2_{QCD}$. The method takes into account perturbative, as well as, nonperturbative gluonic contributions to this correlator. The perturbative contributions arise by direct calculation of Feynman diagrams, while the non perturbative contributions are associated, as we shall discuss, with vacuum expectations values of the correlators, *i.e.* condensates, and sometimes with direct instanton contributions.

The interpolating currents, consistent with the minimum number of gluon fields, used to study low mass glueballs are the field strength squared ($S = 0^{++}$), the topological charge density (0^{-+}) and the energy-momentum tensors ($T = 2^{++}$): [144]

$$J_S(x) = \alpha_s G^a_{\mu\nu}(x) G^a_{\mu\nu}(x), \tag{44}$$

$$J_P(x) = \alpha_s G^a_{\mu\nu}(x) \widetilde{G}^a_{\mu\nu}(x), \tag{45}$$

$$J^{\mu\nu}_T(x) = - G^a_{\mu\alpha}(x) G^a_{\nu\alpha}(x) + \frac{g^{\mu\nu}}{4} G^a_{\beta\alpha}(x) G^a_{\beta\alpha}(x), \tag{46}$$

where $\widetilde{G}^a_{\mu\nu}(x) = (1/2)\epsilon_{\mu\nu\alpha\beta} G^a_{\alpha\beta}(x)$.

The dispersion relation

$$\Pi(Q^2) = \frac{(-Q^2)^n}{\pi} \int_0^\infty ds \; \frac{\mathrm{Im}\Pi(s)}{s^n(s+Q^2)} + a_0 + a_1 Q^2 + ..., \tag{47}$$

where a_i are substraction constants, allows us to connect the theoretical side of the SR (left hand side) with observed properties of the glueballs introduced through $\mathrm{Im}\Pi(s)$ (right hand side). Conventionally, for the phenomenological part of the SR, the following form for the spectral representation is used,

$$\mathrm{Im}\Pi(s)^{\mathrm{phen}} = \sum_i \pi f^2_{G_i} m^4_{G_i} \delta(s - m^2_{G_i}) + \pi\theta(s - s_0) \; \mathrm{Im}\Pi(s)^{\mathrm{theor}}, \tag{48}$$

which corresponds to a sum over narrow width resonances located at $s_i = M_{G_i}$ plus a continuum at large energy $s > s_0$. In Eq. (48), f_{G_i} is the residue of the i^{th}-glueball state defined by the following matrix element,

$$\langle 0|J_G(0)|G_i\rangle = m^2_{G_i} f_{G_i}. \tag{49}$$

Here, m_{G_i} is i^{th}-glueball mass, s_0 is the continuum threshold and $\Pi(s)^{\mathrm{theor}}$ is the perturbative part of the correlator. This is, of course, a rather simplified model for the physical spectral density. However, it has been shown that such a model gives a rather good description of the mass spectrum for the ordinary hadronic states. One may expect therefore, that such a model can be also used for the extracting of the glueball masses.

Before carrying out the numerical analysis of the SR one usually performs the Borel transformation on both sides of the sum rule

$$\hat{B}\Pi(Q^2) \equiv \lim_{n, Q^2\to\infty} \frac{(-1)^n}{n!} (Q^2)^{n+1} \left(\frac{d}{dQ^2}\right)^n \Pi(Q^2)\Big|_{Q^2/n = M^2 = \mathrm{fixed}}$$

where M is called the Borel mass which represents the scale $\tau = 1/M$ in Euclidean time between the two currents in the correlator, Eq. (43).[145] The Borel transformation of the sum rules has two major advantages. The first,

it produces an enhancement of the glueball pole contribution in the right hand side of the SR and, the second, it suppresses, in the theoretical left hand side of the SR, the contribution from the higher power corrections, which arise from high dimension condensates.

The main point of the QCD SR philosophy is the implementation of the interaction of the high virtual valence quark-gluon system with the soft vacuum quark and gluon fields, whose strength is determined by the values of the vacuum condensates. The condensates carry very important information about the long-range quark and gluon field fluctuations in the QCD vacuum. The usual assumption is that one can calculate the hard part within perturbative QCD and the soft part can be parameterized in terms of condensates. It has been demonstrated that, within the OPE approach, in general, the contribution of only a few low dimension condensates is sufficient to describe rather well the properties of the ground hadronic states.[72] However, it was found, many years ago, that in some specific channels, which include the quark-gluon subsystem in a spin zero state, the standard OPE expansion does not work and one needs to incorporate more precise information about the structure of the short-range gluonic fluctuations in the QCD vacuum.[67, 73, 74] The most promising candidate for those short-range fluctuations are instantons (see ref. [75]). The instantons describe tunneling processes which rearrange the QCD vacuum topology in localized space-time regions small enough to affect the x-dependence of the correlators over distances $|x| \ll \Lambda_{\rm QCD}^{-1}$. The average size of instantons in the QCD vacuum is small $\rho_c \approx 0.3$ fm. Therefore, the energy scale related to instanton effects is rather large, $m_I = 1/\rho_c \approx 600$ MeV$\approx 3\Lambda_{\rm QCD}$. Due to such large scale, instantons influence strongly not only the dynamics of the low mass pseudoscalar and scalar mesons, but also the properties of the baryon octet and multiquark states.[76, 77, 78] It has been shown that specific instanton induced quark-quark, quark-gluon and gluon-gluon interactions arising from intermediate distances between hadron constituents can be responsible for various observed features in hadron spectroscopy and hadron reactions.[75, 79, 80, 81] The new ingredient within QCD SRs related to instantons, the so-called direct instanton contribution, provides exponential terms, $\sim \exp(-2Q\rho_c)$ in the expansion of the correlator, in addition to the power terms, $\sim 1/Q^n$, arising from the standard OPE.

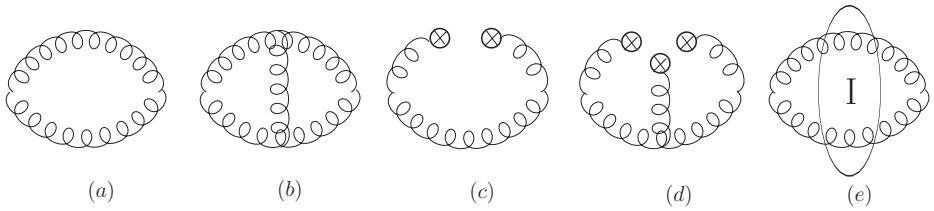

FIG. 6: The diagrams (a) and (b) represent pQCD contributions, diagram (c) represents the contribution arising from the gluon condensate, diagram (d) is the contribution from three-gluon condensate and diagram (e) is the direct instanton contribution.

Finally, the theoretical part of the SR includes the following terms (see Fig. 6)

$$\Pi^{\rm theor}(Q^2) = \Pi^{\rm pert}(Q^2) + \Pi^{\rm cond}(Q^2) + \Pi^{\rm inst}(Q^2). \tag{50}$$

The first two terms in Eq. (50) are calculated using Feynman rules giving for the perturbative part for the correlator of the gluonic field strength[71]

$$\langle TG^a_{\mu\nu}(x)G^b_{\alpha\beta}(0)\rangle_{\rm pert} = -i\delta^{ab}\int \frac{d^4p}{(2\pi)^4)}\Gamma_{\mu\nu\alpha\beta}(p)e^{-ipx}, \tag{51}$$

where

$$\Gamma_{\mu\nu\alpha\beta}(p) = p_\mu p_\nu g_{\alpha\beta} + p_\nu p_\beta g_{\mu\alpha} - p_\mu p_\beta g_{\nu\alpha} - p_\nu p_\alpha g_{\mu\beta}.$$

The term associated to the vacuum condensates is evaluated in the so-called fixed point gauge. In this gauge the soft vacuum gluonic field can be represented by the field strength

$$A^a_\mu(x)_{\rm cond} \approx \frac{x^\nu}{2} G^a_{\nu\mu_{\rm cond}}(0). \tag{52}$$

Using that the QCD vacuum is colorless and Lorenz invariant, and Eq. (52), one obtains the contribution of the vacuum condensates to the OPE for the gluonic channels. It turns out proportional to the value of gluon condensates,

$$\langle\alpha_s G^2\rangle = \langle\alpha_s G^a_{\mu\nu}G^a_{\mu\nu}\rangle, \quad \langle g_s G^3\rangle = \langle g_s f^{abc}G^a_{\mu\nu}G^b_{\nu\rho}G^c_{\rho\mu}\rangle. \tag{53}$$

Unfortunately, the values of the gluonic condensates are not well known. Even the lowest dimension gluon condensate $\langle\alpha_s G^2\rangle \approx 0.035$-$0.075$ GeV^4 is fixed by considering the SRs for quark systems and has large uncertainties (see discussion

in ref. [82]). Other gluonic condensates have been estimated using models for the QCD vacuum. For example, the tree gluon condensate within single-instanton approximation is quite small $\langle g_s G^3\rangle \approx 0.27$ GeV^2 $\langle \alpha_s G^2\rangle$. Lattice calculations are also uncertain. For the lowest dimension condensate the quenched value, $0.14 \pm .02$ GeV^4, is about one order of magnitude bigger than the unquenched one, $0.022 \pm .005$ GeV^4.[83] The uncertainties in the condensate values lead to effects of the order of at least 20% in the extracted masses for glueballs.

The direct instanton contribution is calculated by going to the Euclidian space-time and by introducing in the correlator (43) the instanton field strength, which in the regular gauge has the following form

$$G_{\mu\nu}(x, x_0) = -\frac{\eta_{a\mu\nu}\rho^2}{g_s((x-x_0)^2+\rho^2)^2}, \tag{54}$$

where x_0 is the position of center of instanton and $\eta_{a\mu\nu}$ are the numerical t'Hooft symbols. To get the final result one should also integrate over instanton position, size and orientation.

Let us study in some detail the scalar glueball groundstate, $J^{PC} = 0^{++}$, which would be an ideal state to find since it has many fundamental connotations.[66, 84, 85, 86, 87] In gluodynamics, as we have seen, the situation that arises from lattice calculations is clear and the masses of the scalar glueballs are large $m > 1$ GeV. However, when sea quarks are considered no firm conclusion about the scalar spectrum can be drawn. The theoretical calculations based on QCD SRs and/or low energy theorems lead to contradictory results. Its properties, *i.e.*, mass, decay channels and widths still differ among the various approaches. Dominguez and Paver [88], Bordes, Peñarrocha and Giménez [89], and Kisslinger and Johnson [90], obtain, using low energy theorems and/or SR calculations with (or without) instanton contributions, a low lying and narrow scalar glueball (mass < 700 MeV and $\Gamma_{\pi\pi} < 100$ MeV). Narison and collaborators [91, 92], using two (substracted and unsubstracted) SRs, get a broader (200-800 MeV), heavier (700-1000 MeV) scalar glueball in this range, whose properties imply a strong violation of the Okubo-Zweig-Iizuka's rule. In a recent SR calculation, Forkel [93], obtains the scalar glueball at 1250 ± 200 MeV. However, he has some strength at lower masses which he is not able to ascribe to a resonance in the fits.

Having made these comments let us now see how a calculation proceeds and we let the details of the various approaches just described for the reader to make his own opinion. The calculation we describe is in line with the work of Forkel.[93]

In this case the perturbative contribution arising from Fig. 6(a) and (b) is proportional to a high power of the Q

$$\Pi^{\rm pert}(Q^2) = (\frac{\alpha_s}{\pi})^2 Q^4 \log(Q^2/\mu^2)(A_1 + \frac{\alpha_s}{\pi}A_2), \tag{55}$$

where A_i are some numbers. Therefore, one needs to apply three substractions to have convergence for the dispersion relation[94]

$$\Pi^{theor}(Q^2) = \Pi(0) + Q^2\Pi'(0) + \frac{1}{2}Q^4\Pi''(0) - \frac{Q^6}{\pi}\int_0^\infty ds \frac{{\rm Im}\Pi(s)}{s^3(s+Q^2)} \tag{56}$$

The SRs for the following Borel transforms

$$B_\kappa(\tau) = \frac{1}{\tau}\hat{B}[(-1)^\kappa Q^{2\kappa}\Pi(Q^2)] \tag{57}$$

are

$$\begin{aligned} B_{-1} &= -\Pi(0) + \frac{1}{\pi}\int_0^\infty \frac{ds}{s} e^{-s\tau}{\rm Im}\Pi(s) \\ B_\kappa &= \frac{1}{\pi}\int_0^\infty ds s^k e^{-s\tau}{\rm Im}\Pi(s), \quad \kappa > -1. \end{aligned} \tag{58}$$

After moving the contribution from continuum to the left hand side (theoretical part) of the SR we have

$$\begin{aligned} S_{-1}(\tau, s_0) &= -\Pi(0) + \frac{1}{\pi}\int_0^{s_0} \frac{ds}{s} e^{-s\tau}{\rm Im}\Pi(s) \\ S_\kappa(\tau, s_0) &= \frac{1}{\pi}\int_0^{s_0} ds s^k e^{-s\tau}{\rm Im}\Pi(s), \quad \kappa > -1. \end{aligned} \tag{59}$$

Finally the SRs become

$$\begin{aligned} S_{-1}(\tau, s_0) &+ \Pi(0) = \sum_i f_{G_i}^2 m_{G_i}^2 e^{m_{G_i}^2\tau} \\ S_\kappa(\tau, s_0) &= \sum_i f_{G_i}^2 m_{G_i}^{2\kappa+4} e^{m_{G_i}^2\tau}, \quad \kappa > -1. \end{aligned} \tag{60}$$

Usually the lowest κ value SRs are used to extract the value of glueball mass because they are more stable with respect to the continuum threshold

$$\begin{aligned} m^2 &= \frac{S_1(\tau, s_0)}{S_0(\tau, s_0)} \\ m^2 &= \frac{S_0(\tau, s_0)}{S_{-1}(\tau, s_0) + \Pi(0)}. \end{aligned} \tag{61}$$

In principle, one should obtain the same mass for the glueball in the above two SRs. It was found that the extracted masses for the scalar glueball are quite different in the two. However, as a recent analysis shows, if one includes the direct instanton contribution the mass arising from the two SRs is the same.[93, 95, 96]

These works also suggest a prominent role of the instantons in the binding of the 0^{++} glueball and show relations between the main properties of the 0^++ glueball (mass and size), and the bulk features of the instanton distribution.

In the meantime, the study of instanton contributions to SRs has been extended to other glueball channels.[93, 96] While direct instanton contributions are expected to be small in the tensor channel (mainly due to the absence of the leading correction with respect to the small packing fraction of instantons in the QCD vacuum), they turn out to be also important in the pseudoscalar channel. However, we should stress that the instanton effects are counterbalanced in the pseudoscalar channel by a screening of the topological charge.[93] This screening occurs when the quark contribution is important and leads to a prediction consistent with a low energy theorem. The most accurate result , along these lines, for the masses of the scalar (S) and pseudoscalar (P) glueballs including direct instanton effects in traditional SR calculations is

$$m_S \approx 1.25 \text{ GeV}, \quad m_P \approx 2.2 \text{ GeV}.$$

Within the uncertainties of the QCD sum rule approach these values are in agreement with lattice calculation, which are quenched calculations. Note that the SR predictions include sea quark effect and thus one should be very careful when comparing with the quenched lattice results. In the quenched approximation, the topological charge screening disappears and the instanton effect in the SR for the pseudoscalar glueballs is bigger.

We should emphasize that one central problem of glueball spectroscopy, namely the mixing between quarkonium and the spin zero glueball states still has not been solved so far. Recently, some steps have been done in this direction,[97, 99] and it has been shown that the instantons induce a strong mixing between the two states.[146] In this respect we would like to point out that from our point of view, the tensor 2^{++} glueball channel is the most clean gluonic channel. Indeed, for this state the leading instanton contribution is zero, as follows from the structure of the interpolating current for this channel, which is proportional to the energy-momentum tensor, Eq. (46), and from the fact that the instanton is a vacuum gluon field with zero energy. Therefore, one can expect very small tensor glueball mixing with quarkonium and, as a consequence, a small width for this state and thus the possibility to separate it from the tensor quarkonium states. The SR prediction for the mass and decay constant of 2^{++} state is [100, 101]

$$m_T \approx 2.00 \text{ GeV}, \quad \Gamma_{T\to\pi\pi+KK+\eta\eta} < (119 \pm 36) \text{ MeV}.$$

Due to absence of big uncertainties in the direct instanton contribution and the small expected mixing with quarkonium states in this channel, this SR prediction is on more solid ground than the those for the zero spin glueball states.

V. GLUEBALL PRODUCTION AND DECAYS

One of the most striking features of QCD is the prediction that glueballs might exist, a prediction which has proven difficult to verify. We have seen how different theoretical approaches describe their properties, and now we are going to discuss possible scenarios for their experimental production and detection.

The strategy relies on a very few assumptions. Glueballs are extra states, beyond the $\bar{q}q$ spectrum. To exploit this we must understand the "ordinary" $\bar{q}q$ spectrum very well, using data from J/ψ, B, and Z decays, and from $\bar{p}p$, πp, $\gamma\gamma$, and γN scattering. Glueballs are flavor singlets so their decays should be $SU(3)_F$ symmetric, if the effects of violation of $SU(3)_F$ symmetry are small. Since hybrid and $q\bar{q}\bar{q}q$ states are also "extra" states and some are flavor singlets, the only distinguishing property unique to glueballs is their strong coupling to the color singlet digluon channel.

A convincing way to see a glueball would be to detect a resonance whose quantum numbers are not possible for mesons composed of quark and antiquark, *e.g.* $J^{PC} = 0^{--}, 0^{+-}, 1^{-+}, 2^{+-}$. These glueballs are sometimes called oddballs. They are predicted to be rather narrow and easy to identify experimentally.[102] These states seem to

appear for very large masses. The lightest oddball with $J^{PC} = 2^{+-}$ and a predicted mass of 4.3 GeV will be within range of the future experimental program at $\overline{\mathrm{P}}$ANDA.[103] It is conceivable that comparing oddball properties with those of non-exotic glueballs will reveal deep insight into the glueball structure since their spin structures are different. However, if oddballs happen to appear at lower masses we cannot rule out a glueball interpretation but they should be strongly mixed with hybrid mesons.

However, even non exotic glueballs can be identified by measuring an overpopulation of the experimental meson spectrum and by comparing masses, quantum numbers and decay channels, with predictions from models or lattice QCD. The best scenario is to look for Zweig forbidden processes, since the decay into glueballs is dominant in these cases.[104] These processes are known under the name of gluon-rich processes, some are depicted in Fig. 7. Let us specify some of the processes that fulfil these requirements and are optimal experimental scenarios to search for glueballs:

(i) **J/ψ decays:** the most suggestive process is the radiative J/ψ decay. The J/ψ is narrow; the $D\bar{D}$ threshold is above the mass of the J/ψ and the OZI rule suppresses decays of the $c\bar{c}$ system into light quarks. In most decays, the J/ψ undergoes a transition into 3 gluons which then convert into hadrons. This is a high multiplicity process difficult to detect. But J/ψ can also decay into 2 gluons and a photon. The photon can be detected, the two gluons interact and must form glueballs. BES III will provide huge J/ψ data samples allowing definitive studies of J/ψ decay and, especially, partial wave analysis of the glueball-preferred radiative J/ψ decay channel.[105]

(ii) **Central production:** glueballs decay into hadrons and hence hadro-production of glueballs is always possible. Central production is a process in which glueballs should be abundantly produced.[106] In central production two hadrons scatter diffractively, gluon-gluon fusion processes should be abundant and no valence quarks are exchanged. The process is often called double pomeron exchange, with the pomeron presumed to be a multi-gluon color singlet. The absence of valence quarks in the production process makes central production a good place to search for glueballs.

(iii) $\bar{p}p$ **annihilation:** quark-antiquark pairs annihilate into gluons, they interact and may form glueballs, *e.g.* $\bar{p}p \to \pi^0 G$. A new era of precise experiments will start when $\overline{\mathrm{P}}$ANDA starts to operate.[103]. The energy range of this experimental program will allow the study of oddballs. Glueballs can either be formed directly in the $\bar{p}p$-annihilation process, or produced together with another particle. In both cases the glueball decay into final states like $\phi\phi$ or $\phi\eta$ would be a favorable reaction below 3.6 GeV, while J/$\psi\eta$ and J/$\psi\phi$ are the first choice for more massive states.

(iv) $\gamma\gamma$ **fusion:** production of glueballs should be suppressed in this case since photons couple to the intrinsic charges. So we should expect a glueball to be strongly produced in radiative J/ψ decays but not in $\gamma\gamma$ fusion. Radial excitations might be visible only weakly in J/ψ decays but they should couple to $\gamma\gamma$. However, if a very low mass glueball would exist, this would be one of the cleanest ways to find it in a difficult experiment due to the low counting rate.

(v) **photoproduction:** it has been a continuous source of meson resonances. Photoproduction is expected to be particularly effective in producing exotic hybrids and glueballs. The photon, *via* Pomeron exchange from the vacuum, or *via* its hadronic component, can create states with exotic J^{PC}. These mesons can be hybrids, glueballs or mixed states. Moreover, also non exotic hybrid (glueball) states can be produced which manifest themselves as extraneous states that cannot be accommodated within $\bar{q}q$ nonets. However, there is little data on photoproduction of light mesons. This will drastically change when the GlueX experiment goes into operation, since it is designed to collect data of unprecedent statistics and quality.[107] Moreover, the (linear) polarization of the beam will allow the identification of (exotic) quantum numbers and the determination of the details of the production mechanism of (glue) mesons.

The status of glueball observation would become clearer with a combination of data of pp and e^+e^- machines with large statistics, however since the glueball width into two-photons is small, this would require very high luminosity. It has been pointed out that heavy-ion colliders, due to their large center of mass energy, allow access to the Regge region $s \gg |t|$ and hence to the production of glueballs in peripheral collisions through photon-photon collisions as well as double pomeron exchange [108, 109, 110].

Distinctive features can be derived from the decays of the glueballs since they are flavour singlets: decays to $\eta\eta'$ identify a flavour octet and radiative decays of glueballs are forbidden. However, these arguments have to be taken with care since mixing of a glueball with mesons, having the same quantum numbers, can occur and would dilute any selection rule.

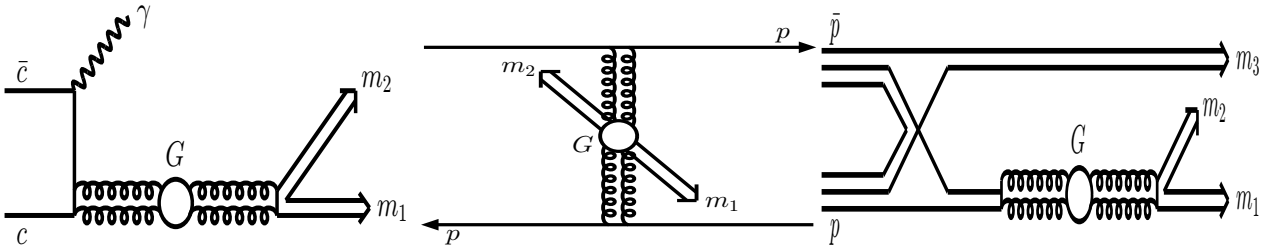

FIG. 7: Diagrams possibly leading to the formation of glueballs: radiative J/ψ decays, pomeron-pomeron collisions in hadron-hadron central production, and in $p\bar{p}$ annihilation.

An interesting idea recently proposed is that of chiral suppression.[111] If chiral symmetry breaking in glueball decay is dominated by quark masses, then the coupling of a spin zero glueball to light $q\bar{q}$ pairs is chirally suppressed. An interesting consequence is that radiative J/ψ decay becomes a filter for new physics in the $J = 0$ channel, since at leading order radiative decays to spin zero light quark mesons are suppressed while radiative decays to $J = 0$ glueballs, hybrid, and four quark states are not suppressed. This idea is not without controversy. [112, 113]

The glueball groundstate $J^{PC} = 0^{++}$ would be an ideal state to find since it has many fundamental connotations.[66, 84, 85, 86, 87] In gluodynamics, as we have seen, the situation that arises from lattice calculations is clear and the masses of the scalar glueballs are large $m > 1$ GeV. However, when sea quarks are considered no firm conclusion about the scalar spectrum can be drawn. The theoretical calculations based on QCD sum rules and/or low energy theorems lead to contradictory results. Its properties, *i.e.*, mass, decay channels and widths still differ among the various approaches.

Experimentally there are too many isoscalar, scalar mesons between 0.6 and 1.75 GeV to be explained by the naive quark model alone. From the theoretical point of view there has been a lot of debate about the structure of these states. Let us summarize here the different theoretical explanations for the spectrum. Jaffe obtains the $f_0(600)$ and the $f_0(980)$ in the bag model as cryptoexotic $q\bar{q}\bar{q}q$ states.[114] The p-wave $q\bar{q}$ scalar nonet is likely to lie in the region of the other spin-triplet p-wave nonets, with isoscalars roughly between ~ 1250 and ~ 1600 MeV. [13] Dominguez and Paver,[88] Bordes, Peñarrocha and Giménez,[89] and Kisslinger and Johnson,[90] obtain, using low energy theorems and/or sum rule calculations, a low lying and narrow glueball (mass < 700 MeV and $\Gamma_{\pi\pi} < 100$ MeV). Vento using low energy theorems has also proposed the existence of a low mass ($m < 700$ MeV) and almost sterile scalar glueball.[87] Narison and collaborators,[91, 92] using sum rules, get a broader (200-800 MeV), heavier (700-1000 MeV) scalar glueball in this range. Forkel,[93] obtains a scalar glueball at 1250 ± 200 MeV with a large width ($\sim$300 MeV). Between ~ 1400 and 1750 MeV there are three $I, J^{PC} = 0, 0^{++}$ states: $f_0(1370)$, $f_0(1500)$, and $f_0(1710)$. In the analysis of Vento [87] two scalar glueballs appear in this range, an intermediate mass glueball (~ 1300 MeV) and another one in the upper range ($\sim 1500 - 1700$ MeV). The narrow state at 1500 MeV, discovered in $p\bar{p}$ annihilation by Crystal Barrel (CB) is considered by Amsler and Close a good candidate for the glueball groundstate[13, 115, 116] while Chanowitz considers the $f_0(1710)$ as the scalar groundstate[14, 111]. Finally, that the scalar glueball is shared by both resonances is also contemplated.[14]

VI. GLUEBALLS AND THE QUARK-GLUON PLASMA

Relativistic heavy-ion collisions might be a tool to produce glueballs. It is conceivable that glueball production becomes a dominant part in central nucleon collisions.

Two scenarios will be analyzed:

(i) **Quark Gluon Plasma phase**: one expects that at some point above a certain critical temperature a plasma of quarks and gluons, named quark-gluon plasma (QGP) is formed.[117] This phase is characterized by a large amount of thermal gluons. As the QGP cools down the gluons can form singlet configurations via the color interaction.

(ii) **Strong Coulomb phase**: a recent formulation of the dynamics in the region above the transition temperature T_C, based on a description of recent experiments in ultra relativistic heavy ion collisions,[118] states that, despite de-confinement, the color Coulomb interaction between the constituents is strong and a large number of binary (even color) bound states, with a specific mass pattern, are formed.[119] This phase we call Strong Coulomb Phase (SCP). The QGP phase occurs at a much higher temperature $T_{QGP} > (2-3)T_C$ when the bound states dissolve.

Let us describe some attempts to find signatures arising from QGP. The basic idea is that during the hadronization process in this gluon rich environment the gluons combine due to the strong force into glueballs. As the QGP cools further and transforms into hadronic matter, these glueballs decays into conventional hadrons giving rise to signatures of their existence. It has been claimed that the existence of glueballs alters the K/π ratio in the final state.[120]

It is conceivable that glueball production becomes dominant in central nuclear collisions since the existence of QGP provides a gluon rich environment especially at high energy density. In this scenario the lowest mass glueballs are copiously produced. Particular decay modes $0^{++}, 2^{++} \to K\bar{K}$ and $0^{++} \to \pi^+\pi^- l^+ l^-$ have been investigated[121] and enhancements associated with possible glueball production observed. Search strategies, including dipion production have been also proposed.[122]

Estimates within thermal models for the multiplicities of scalar glueballs in central Au-Au collisions at present and future experimentally available energies, *i.e.* from AGS to LHC, have been presented.[123] For the experimental identification of glueballs one can use the decay modes $G \to K\bar{K}$, $G \to \gamma\gamma$ and $G \to 2\pi l^+ l^-$. Despite of small branching ratio, the 2γ channel has the important advantage that photons have practically no rescattering in the hadronic medium. This analysis leads to maximal multiplicities for the glueball of $1.5-5\%$ of the ϕ meson multiplicity. Even larger yields are expected in the case of explosive hadronization of the quark gluon plasma.[123]

Let us now turn to the second scenario. From its inception two decades ago, the high-T phase of QCD commonly known as the Quark-Gluon Plasma,[117] was described as a weakly interacting gas of "quasiparticles"(quarks and gluons). Indeed, at very high temperatures asymptotic freedom causes the electric coupling to be small and the QGP to be weakly interacting. At intermediate temperatures of few times the critical temperature T_c of immediate relevance to current experiments, there is new and growing evidence that the QGP is not weakly coupled. In this region QCD seems to be close to *a strongly coupled Coulomb regime*, with an effective coupling constant $\alpha \approx 0.5$-1 and multiple *bound states* of quasiparticles.[119] This phase we call Strong Coulomb Phase. This description is not universally accepted since some lattice calculations do not to find bound states above the transition.[124, 125] Also, one must be aware that other explanations of the data have been presented.[126] In order to clarify these issues it is interesting to find clear experimental observables that would shed some light into the discussion.

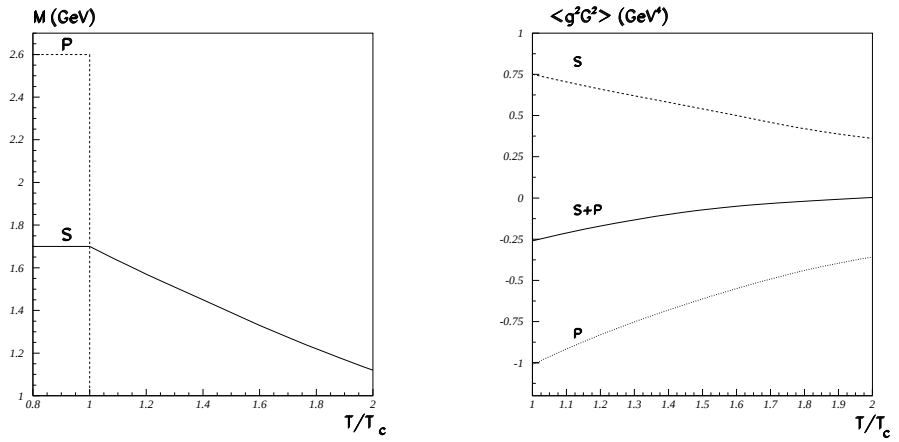

FIG. 8: The solid (dotted) line is the temperature dependence of scalar (pseudoscalar) glueball mass (left).The temperature dependence of the gluon condensate at $T > T_c$. The solid line is total condensate, the dashed (dotted) line is the scalar (pseudoscalar) glueball contributions (right).

Kochelev and Min consider the properties of scalar and pseudoscalar glueballs in SCP.[127] In an effective Lagrangian approach, based on the low-energy QCD theorems, they find out that scalar glueball remains massive above deconfinement temperature (see Fig. 8). At the same time, pseudoscalar glueball changes its properties in QGP in a drastic way. Indeed, this glueball becomes massless at $T > T_c$ and therefore it can contribute strongly to,the bulk properties of the plasma (see Fig. 8). They demonstrate that the disappearance of pseudoscalar glueball mass above the deconfinement temperature and its strong coupling to gluons gives the rise to the sign change of the gluon condensate in the pure $SU(3)_c$ gauge theory as observed in the lattice calculations at $T \approx T_c$ (see Fig. 8).[128] The strong nonperturbative coupling of the glueball to the gluons leads to the conjecture that one might expect that the role of very light pseudoscalar glueball in QGP must be quite similar to the role played by the massless pion in nuclear matter below deconfinement temperature.

In SCP despite de-confinement the color Coulomb interaction between the constituents is strong and a large number

of binary (even color) bound states, with a specific mass pattern, are formed.[119] With this input, the scenario envisaged by Vento for gluodynamics, *i.e.* the theory with only gluons goes as follows.[129] The strong Coulomb phase is crowded with gluon bound states and the lightest is the scalar glueball, labelled g. As one moves towards the dilution limit, the binding energy of these states decreases, the gluon mass increases, and therefore the color and singlet bound states increase their mass softly until the gluons are liberated forming a liquid.[119] However, as the system cools towards the confining phase, color and singlet states decay into the conventional low lying glueballs, in particular g. Thus the number of g's becomes large.

This reasoning generalizes to QCD since in the SCP the multiplicity of glueball channels is larger than in the confined phase. The ratio of glueball to meson channels goes from 1 to 8 below the phase transition to 1 to 2 above.[119] Thus the number of scalar glueballs is much larger in SCP than in the cold world.

As the fireball cools a "large number" of gluonic bound states decay by gluon emission into g's. The emitted gluons form new bound states of lower mass due to the strong color Coulomb interaction. As we approach the confinement region the mass of the color bound states increases and it pays off to make multiparticle color singlet states, which decay by rearrangement into ordinary color singlet states. Since the coupling is strong and the phase space is large, these processes take place rapidly. Thus in no time, close to the phase transition temperature T_C, a large number of scalar glueballs populate the hadronic liquid.

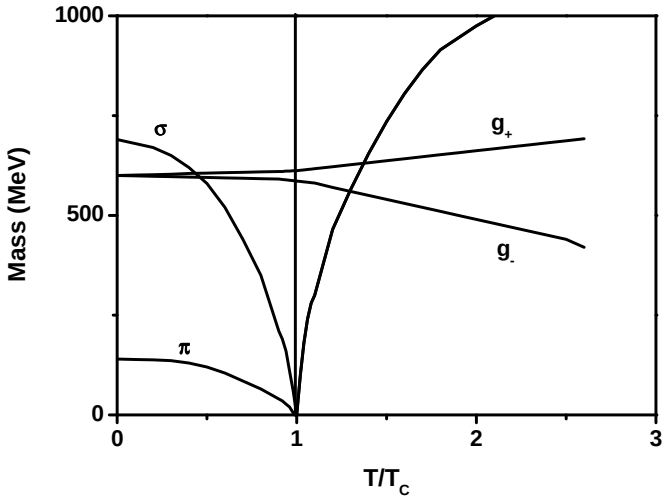

FIG. 9: Behavior of the masses of σ,π and g across the QGP phase transition according to model calculations. $g_\pm$ label the upper(lower) limits of the g in mass model calculations.[130]

Let us now analyze the experimental signal of these phenomenon. If we assume that the σ is the O(4) partner of the π in the chiral symmetry realization of QCD, its mass decreases when approaching the phase transition, becoming degenerate with the pion at T_C (see Fig. 9). Beyond T_C, in the SCP, chiral symmetry is restored, and π and σ remain degenerate for $T > T_C$. Thus in the SCP the σ can only decay in 2γ for obvious kinematical reasons. The glueball g does not vary its mass in this region appreciably. Thus even before we reach T_C, the mixing between g and σ disappears (see Fig. 9) and g becomes stable around T_C. However, in the SCP the mass of the σ increases and in a certain region of T it again becomes degenerate with g and mixing is restored. Thus the physical g is able to decay, once the σ component is attained, only to 2γ.

The enhancement in the number of gs with respect to the hadronic phase arises because of the larger population of glueballs in the SCP, as described above, and because these particles are stable in the medium against the dominating hadronic decays (see Fig. 9). Thus a clear signal for the existence of a low mass scalar glueball and a confirmation of the SCP scenario would be two 2γ peaks corresponding to g and the σ-meson as shown in Fig. 10.

The investigation on jets in the relativistic heavy ion collisions at RHIC provides a deep insight into the properties of the quark-gluon plasma.[118] One of the important RHIC discoveries is the jet quenching phenomenon coming from the partonic energy loss in QGP. In the conventional approach to the jet quenching the perturbative (pQCD) type of energy loss is taken into account by the channels, elastic and radiative, of one-gluon exchange between the jet

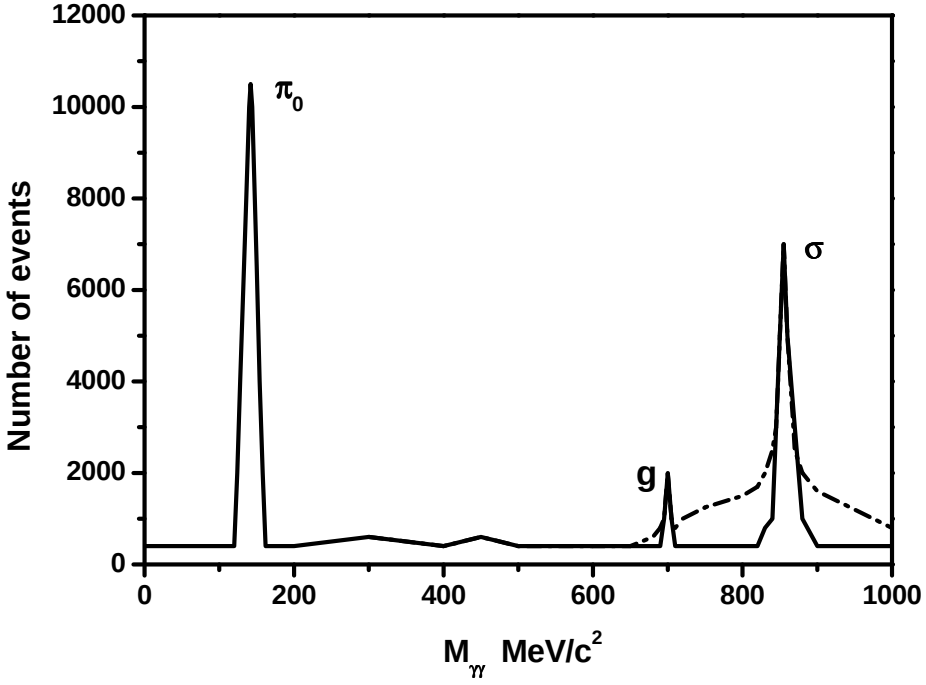

FIG. 10: Expected fit to the two-photon invariant mass spectrum in central Pb-Pb collisions after substraction from the background. The 2γ decays should allow for a clear separation of g and σ. The figure includes an estimate of the effect of the hadronic widths on the fits (dot-dashed line).

and the massless gluons and quarks.[131] However, the large quark-gluon rapidity density $dN_{qg}/dy \approx 2000$ which is needed to describe the RHIC jet quenching data within this approach, seems to be in contradiction with the restriction $dN_{qg}/dy \leq 1/4dS/dy \approx 1300$ coming from the measured final entropy density $dS/dy \approx 5000$.[132] Furthermore, the lattice calculations show that even at very high temperature gluons and quarks still interact strongly in QGP. [128]

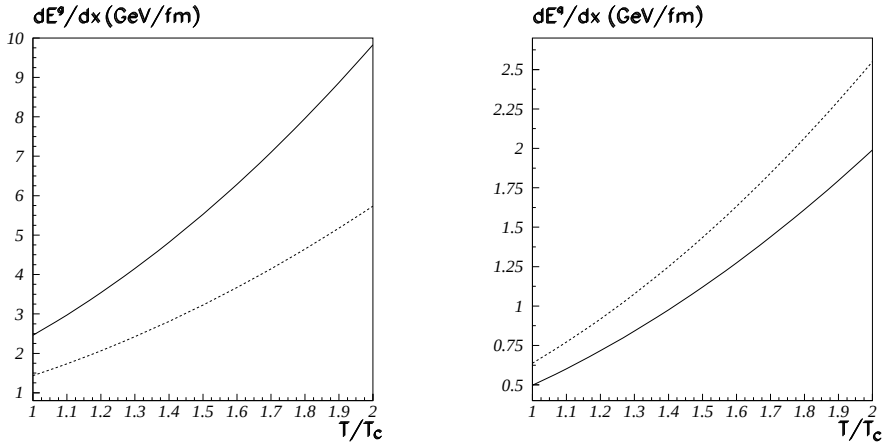

FIG. 11: The temperature dependence of gluon energy loss (left). The temperature dependence of quark energy loss (right).The solid (dashed) line is glueball (pQCD) contribution .

As seen above, it has been suggested that the glueballs, the bound states of gluons, can exist above deconfinement temperature and may play an important role in the dynamic of strongly interacting QGP.[127, 129] In particular, it has been suggested that a very light pseudoscalar glueball can exist in QGP and might be responsible for the residual strong interaction between gluons.[127] The lattice results showing a change of sign of the gluon condensate[128] and a small value of the topological susceptibility above T_c can be explained in the glueball picture as well. Furthermore, one expects that the suppression of the mixing between glueballs and quarkonium states in the QGP leads to a smaller

width for the former as compared to the vacuum.[129] This property opens the possibility for a clear separation of the glueball and the quark states in heavy ion collisions. Such separation is rather difficult in other hadron reactions due to existence of strong glueball-quarkonium mixing in the vacuum.

Min and Kochelev made an estimate of the energy loss induced by interaction of an energetic parton, which was produced in the hard scattering of two heavy ion's partons, with glueballs in the hot quark-gluon plasma.[133] They showed that such contribution leads to a significant energy loss as can be seen from Fig. 11. In particular, for the gluon jet such contribution is about a few GeV/fm and approximately twice larger than the perturbative elastic loss.[134] It should be pointed out that more than one half of contribution to the gluon energy loss comes from interaction of gluon with the light pseudoscalar glueball in QGP. Thus in spite of the fact that for the quark jet the glueball contribution is smaller than perturbative elastic loss, it can not be neglected in comparison with latter one. The existence of such light bound state of gluons above T_C is crucial for the understanding of the large observed partonic energy loss in QGP. Therefore, not only pQCD type of energy loss but also glueball-induced loss, arising from existence of scalar and pseudoscalar glueballs in QGP, are important for the understanding of the RHIC results such as the jet quenching.

VII. OTHER DEVELOPMENTS

A. Glueballs and the Pomeron

It is well known that in the many high energy reactions with small momentum transfer the exchange by the highest-lying Regge trajectory, called as a soft Pomeron, gives the dominant contribution. This exchange carries vacuum quantum numbers and has very peculiar properties in comparison with the usual Regge pole trajectories as the ρ, π, *etc.* From the analysis of the varions cross sections it follows that the Pomeron trajectory has a linear behavior

$$J(t = m^2) = 1.08 + 0.25m^2. \tag{62}$$

The Pomeron does not seem to be related to the usual mesons since the latter have usually lower intercepts and very different slopes. There has been a long-standing speculation that the physical particles on the trajectory might be glueballs.

Meyer and Teper investigated the pure gauge spectrum on a lattice to check its compatibility with a linear trajectory.[18] They calculated the lightest states $J^{PC} = 2^{++}, 4^{++}, 6^{++}$ since the trajectory has an even signature. Their masses (within errors bars) are consistent with the Pomeron trajectory (62). These studies of quarkless QCD helps to understand the close relation between the Pomeron and the pure glue states, but it is worth mentioning that the physical particles should probably mix with quarkonia. The linearity of the trajectory, supported by these arguments, favors flux tube and stringy pictures as discussed in the constituent model section, at least for $(\text{even})^{++}$ glueballs.

B. Glueball - $q\bar{q}$ mixing

Most of our review has been dedicated to the study of pure glueball states. We have assumed in our discussion that glueballs are physical objects, which is fine for the purpose of the developments thus far. But in order to establish contact with reality we have to discuss in some detail mixing, an idea which has been mentioned in passing on several occasions. We first discuss the mathematics of mixing in a two state model and then apply the reasoning to the physical reality in the isosinglet scalar sector.

Mixing arises when the total Hamiltonian is not diagonal in the glueball and $q\bar{q}$ Fock space. In this case the physical states come out as superpositions of glueballs and $q\bar{q}$ states. Let us assume that we have a pure glueball, we label g, and a $q\bar{q}$ state, we label σ, which have the same quantum numbers and, for simplicity, also the same mass m, in a certain approximation. We next relax this approximation and the Hamiltonian in the reduced g and σ Fock space becomes

$$\begin{pmatrix} m & \delta \\ \delta & m + \Delta m \end{pmatrix} \tag{63}$$

The diagonal basis of this Hamiltonian can be presented as,

$$|\tilde{g}\rangle = \cos(\theta/2)|g\rangle - \sin(\theta/2)|\sigma\rangle, \tag{64}$$

$$|\tilde{\sigma}\rangle = \sin(\theta/2)|g\rangle + \cos(\theta/2)|\sigma\rangle, \tag{65}$$

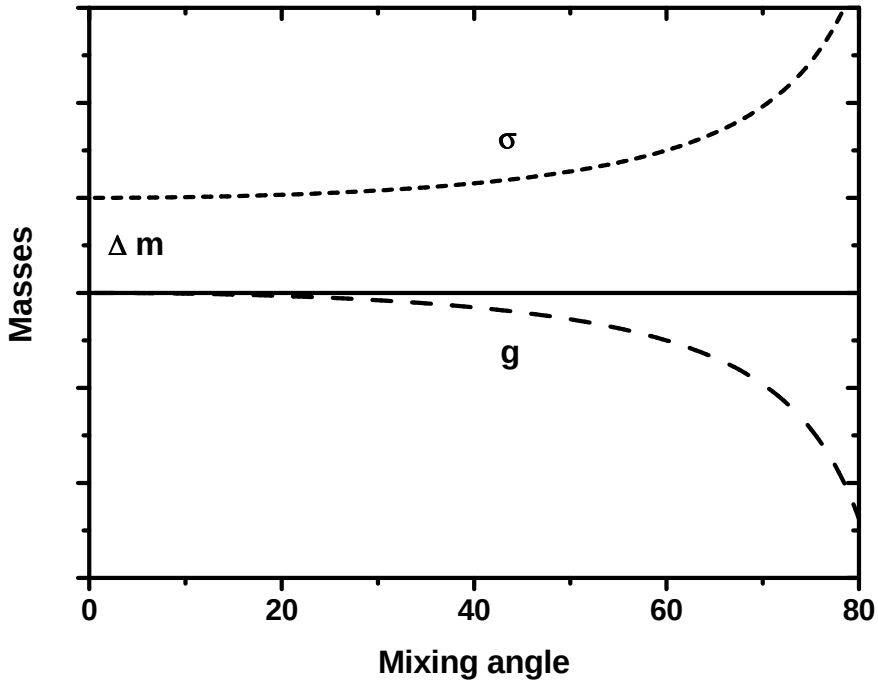

FIG. 12: The limiting values for the masses of the physical g (solid–dashed lines) and σ (solid–short-dashed lines) are shown as a function of the mixing angle.

where the tilde labels the physical particles and θ is the mixing angle.

The masses of the physical particles become

$$m_{\tilde{g}} = m + \frac{\Delta m}{2} - r, \qquad m_{\tilde{\sigma}} = m + \frac{\Delta m}{2} + r, \tag{66}$$

where

$$\tan\theta = \frac{2\delta}{\Delta m} \tag{67}$$

and

$$r = \frac{\Delta m}{2}\sqrt{1 + \left(\frac{2\delta}{\Delta m}\right)^2} = \frac{\Delta m}{2\cos\theta}. \tag{68}$$

In Fig. 12 we represent the masses of the physical states as a function of the mixing angle θ. The curves separate possible mass regions. The curves show that the two state mixing scenario for positive Δm leads to a "light" glueball and heavier meson. The opposite result can be obtained with a negative Δm. The procedure can be generalized to more states and to different initial masses as we next see. This mechanism has been used to try to disentangle the complex isoscalar sector.

Vento has shown that a low mass, almost invisible isosinglet scalar glueball, could hide in the low energy spectrum due to small mixing with the $f_0(600)$, and pointed out the possible existence of other glueballs components among the remaining isosinglet scalars $f_0(1370)$, $f_0(1500)$ and $f_0(1710)$.[87]

Close *et al.* have discussed the content of the the isosinglet scalar mesons $f_0(1370)$, $f_0(1500)$ and $f_0(1710)$ in an attempt to discover which of them is dominantly a scalar glueball.[135, 136] These authors have suggested that $f_0(1500)$ is primarily a scalar glueball, due partly to the fact that $f_0(1500)$, discovered in $p\bar{p}$ annihilation at LEAR, has decays to $\eta\eta$ and $\eta\eta'$ which are relatively large compared to that of $\pi\pi$[137] and that the earlier quenched lattice calculations[9, 138] predict the scalar glueball mass to be around 1550 MeV. Furthermore, because of the small production of $\pi\pi$ in $f_0(1710)$ decay compared to that of $K\bar{K}$, they claim that the $f_0(1710)$ is primarily $s\bar{s}$ dominated. In contrast, the smaller production rate of $K\bar{K}$ relative to $\pi\pi$ in $f_0(1370)$ decay leads to the conjecture

that $f_0(1370)$ is governed by the non-strange light quark content. Based on these observations, they have proposed a flavor-mixing scheme to consider the glueball and $q\bar{q}$ mixing in the neutral scalar mesons $f_0(1710)$, $f_0(1500)$ and $f_0(1370)$.[135] Fits to the measured scalar meson masses and their branching ratios of strong decays have been performed in several[135, 136, 139] leading to a mixing matrix of the form

$$\begin{pmatrix} f_0(1370) \\ f_0(1500) \\ f_0(1710) \end{pmatrix} = \begin{pmatrix} -0.91 & -0.07 & +0.40 \\ -0.41 & +0.35 & -0.84 \\ +0.09 & +0.93 & +0.36 \end{pmatrix} \begin{pmatrix} |N\rangle \\ |S\rangle \\ |G\rangle \end{pmatrix},$$

where $|N\rangle$ and $|S\rangle$ denote the quarkonium states $(|u\bar{u}\rangle + |d\bar{d}\rangle)\sqrt{2}$ and $|s\bar{s}\rangle$, and $|G\rangle$ denotes the pure scalar glueball state. Thus for Close *et al.* the $f_0(1500)$ is composed primarily of a scalar glueball.

Another analysis has been carried out by Cheng *et al.*.[140] Two lattice results are employed as the starting point; one is the approximate SU(3) symmetry in the scalar sector above 1 GeV for the connected insertion part without $q\bar{q}$ annihilation,[141] and the other is the scalar glueball mass at 1710 MeV in the quenched approximation.[17, 19] In the SU(3) symmetry limit, $f_0(1500)$ becomes a pure SU(3) octet and is degenerate with $a_0(1450)$, while $f_0(1370)$ is mainly an SU(3) singlet with a slight mixing with the scalar glueball which is the primary component of $f_0(1710)$. These features remain essentially unchanged even when SU(3) breaking is taken into account. The observed enhancement of $\omega f_0(1710)$ production over $\phi f_0(1710)$ in hadronic J/ψ decays and the copious $f_0(1710)$ production in radiative J/ψ decays lend further support to the prominent glueball nature of $f_0(1710)$. Furthermore, chiral suppression[27, 111, 142] is advocated to obtain the following mixing matrix,

$$\begin{pmatrix} f_0(1370) \\ f_0(1500) \\ f_0(1710) \end{pmatrix} = \begin{pmatrix} +0.78 & +0.51 & -0.36 \\ -0.54 & +0.84 & +0.03 \\ +0.32 & +0.18 & +0.93 \end{pmatrix} \begin{pmatrix} |N\rangle \\ |S\rangle \\ |G\rangle \end{pmatrix}.$$

Therefore for Cheng *et al.* it is the $f_0(1710)$ is the particle composed mostly of a glueball state. Thus a definitive conclusion on this problem is still lacking.

Finally we would like to mention that the quarkonium-glueball mixing gives also a strong influence to the properties of the lowest mass pseudoscalar glueball.[97, 143]

VIII. CONCLUSIONS

The leitmotif of this review has been that the study of glueballs, states where the gauge field plays an important dynamical role, is important to understand the nonperturbative behavior of QCD. This study requires precise and abundant experimental input, which despite a lot of effort has not achieved a level of understanding that allows a unique theoretical interpretation. The lack of clarity arises from the fact that the theoretical developments are not able to determine in a well defined manner how the production and decay properties of glueballs are distinct from those of conventional mesons. But the future is bright for several reasons. New energy domains will be studied by BESIII and in the future by $\overline{\text{P}}$ANDA, and therefore the possibility of producing oddballs, glueballs with exotic quantum numbers will open. Moreover, at low energy, both Crystal Barrel and in the future GlueX will produce light mesons with a level of statistics, and precision for analysis, that will be able to separate exotic from non exotic behaviors and quark model nonets from particles extraneous to them. In this process the new theoretical developments will be crucial to guide and/or interpret the results.

In this review we have discussed three major approaches, lattice QCD, QCD based constituent models and QCD sum rules, with a short excursion into the AdS/QCD formalism, which at present leads ultimately to a constituent model type of description.

Due to the lack of observable states, the lattice QCD results have played the role of experimental data. Lattice QCD is a powerful technique, especially for the determination of masses. The spectrum of the pure gluodynamics (the pure gauge theory), equivalent to the so called quenched approximation of lattice QCD, is well established and the calculational errors are under control. However the various treatments of quark loops (unquenched lattice QCD) and the effects of the mixing of glueballs with mesons are still a matter of debate and no firm conclusions can be drawn for the real world. Moreover, important features of the study would be the determination of the decay properties of the various glueball candidates, and lattice QCD being a theory described in Euclidean space-time does not possess the capability of describing asymptotic states and therefore of determining decay properties. However, a full lattice QCD calculation with unlimited and precise calculational power should produce the experimental spectrum, if as we strongly believe QCD is the theory of the hadronic interactions, and moreover, if one can extend lattice QCD into Minkowski space-time one would be able to determine the decay properties.

Given the lack of experimental and detailed theoretical knowledge, models turn out to be an interesting laboratory to test ideas of the various perturbative and nonperturbative mechanisms in the theory. We have discussed in some detail constituent gluon models for glueballs from different perspectives. Most of the pioneer work considered glueballs as strongly bound states of two (or three) heavy spin-1 gluons. The comparison with lattice QCD shows that the spectrum obtained by these approaches does not correspond to lattice QCD. However, if one implements a formalism dealing with only transverse gluons, the spurious states (induced by the gluonic longitudinal components) disappear and the hierarchy in the spectrum of lattice QCD is recovered. These improvements have been developed up to now only in the two-gluon sectors and the generalization to negative C-parity is still lacking. It remains for the future to find out which constituent glueball model confirms the lattice QCD spectrum for the higher states.

The dynamics in these models is described, in general, by a linear plus Coulomb potentials. This dynamics, however, does not remove the degeneracy of the scalar and pseudoscalar glueballs. The candidate instanton induced interaction, which arises naturally in QCD and which has very particular properties under spin-parity, is the natural candidate to do the job. In the quenched approximation, the instanton induced interaction is attractive in the scalar and repulsive in the pseudoscalar channels, and equal in magnitude. This is the precise behavior needed to lift the degeneracy in the constituent models.

The QCD sum rules offer the possibility to describe mixing and sea quarks effects in glueball states. The method is rather technical and requires many ingredients (condensates, instantons, topological charge screening, ...). This complexity has led to many different calculations, with different results for the lowest lying states. We refer the reader to the literature for the various attempts to describe the low mass glueball spectrum. In here, we present the general formalism and some details of a specific calculation, in which the masses are obtained from pure gluonic currents, however, sea quarks effects are included (*via* the quark condensate).

Glueballs should be produced preferably in gluon-rich processes. We described briefly the main examples: J/ψ decays, central production $\bar{p}p$ annihilation,$\gamma\gamma$ fusion and photoproduction. The realization of a new generation of experiments, BESIII, $\overline{\text{P}}$ANDA and GlueX, provide hope for new exciting developments in this field.

The ultra-relativistic heavy ion experiments is another experimental scenario where one expects that glueballs might play a role. It is clear that the transition to a different phase of confinement, be it the Strong Coulomb phase or the Quark Gluon Plasma, precludes that the confinement properties of the bound systems will change and with it their physical behavior. There is no consensus on the glueball properties above the critical temperature and this has led to the description of several scenarios which can be very interesting from the point of view of observation. RHIC has produced large amount of date at high temperature, as will very soon do ALICE. On the other hand FAIR will probe the high density region. Given these circumstances it is clear that the aim is to performed realistic analysis which are are able to disentangle the right from the wrong ideas.

Finally, the strong expected mixing between glueballs and quark states leads to a broadening of the possible glueball states which does not simplify their isolation and their theoretical description. The wishful sharp resonances which would confer the glueball spectra the beauty, richness and simplicity of the conventional baryonic and mesonic spectra are lacking. We hope that in the future and at higher energies the situation changes and we are able to have isolated exotic states. It is, however, important to stress, that in any case gluebals are a beautiful and unique consequence of QCD.

The study of glueballs is intimately related to the quantitative understanding of confinement in QCD, since understanding confinement requires an understanding of the soft gluonic field responsible for binding the hadrons and the structure of the QCD vacuum. We have emphasized that this has been the goal of the various studies, *i.e.* to get a clearer picture of how QCD behaves at relatively low momentum and how this behavior changes as the temperature or the density increase. Our review shows that we have learned much but we have yet not achieved the goal. We foresee a bright future in this respect since a new experimental era of the study of QCD in many fronts is opening up. To find a description, which is able to describe all the various phenomena in a unique framework, is our task, and when achieved will imply that we finally understand QCD. The venture is even more exciting since maybe AdS gravity might come to our help, a possibility unthinkable a few years back.

Acknowledgements

We would like to thank Philippe de Forcrand, Alexander Dorokhov, Hilmar Forkel, Sergo Gerasimov and Dong-Pil Min for useful discussions. Vincent Mathieu thanks the I.I.S.N. (Belgium) for financial support. Nikolai Kochelev was partly supported by Belarus-JINR grant. This work was done Vicente Vento was on a sabbatical from the University of Valencia at the PH-TH at CERN, whose members he thanks for their hospitality. Vicente Vento was supported by

MECyT-FPA2007 and by MEC-Movilidad PR2007-0048.

[1] H. Fritzsch, M. Gell-Mann and H. Leutwyler, *Phys. Lett.* B47 (1973) 365.
[2] D. J. Gross and F. Wilczek, *Phys. Rev. Lett.* **30** (1973) 1343.
[3] H. D. Politzer, *Phys. Rev. Lett.* **30** (1973) 1346.
[4] K. G. Wilson, *Phys. Rev. D* **10** (1974) 2445.
[5] H. Fritzsch and P. Minkowski, *Nuov. Cim.* **30**A (1975) 393.
[6] R. L. Jaffe and K. Johnson, *Phys. Lett. B* **60**, 201 (1976).
[7] S. Okubo, *Phys. Lett.* **5**, 1975 (1963); G. Zweig, in *Development in the Quark Theory of Hadrons*, edited by D.B. Lichtenberg and S.P. Rosen (Hadronic Press, Massachusetts, 1980); J. Iizuka, *Prog. Theor. Phys. Suppl.* **37**, 38 (1966).
[8] A. Hart and M. Teper, *Phys. Rev. D***65** (2002) 034502; **Nucl. Phys. Proc. Suppl.** 119 (2003) 266.
[9] G.S. Bali et. al., *Phys. Rev. D***62** (2000) 054503; G.S. Bali et al., *Phys. Lett. B***309** (1993) 378.
[10] E. Klempt and A. Zaitsev, *Phys. Rept.* **454**, 1 (2007)
[11] W. Ochs, *Nucl. Phys. Proc. Suppl.* **174**, 146 (2007) [arXiv:hep-ph/0609207].
[12] V. V. Anisovich, M. A. Matveev, J. Nyiri and A. V. Sarantsev, *Int. J. Mod. Phys. A* **20**, 6327 (2005) [arXiv:hep-ph/0506133].
[13] C. Amsler and F. E. Close, *Phys. Lett. B* **353** (1995) 385 [arXiv:hep-ph/9505219].
[14] M. S. Chanowitz, *Int. J. Mod. Phys. A* **21** (2006) 5535 [arXiv:hep-ph/0609217].
[15] F. Giacosa, T. Gutsche, V. E. Lyubovitskij and A. Faessler, *Phys. Rev. D* **72** (2005) 114021 [arXiv:hep-ph/0511171].
[16] C. McNeile, *Nucl. Phys. A* **711** (2002) 303 [arXiv:hep-lat/0207001].
[17] C. J. Morningstar and M. J. Peardon, *Phys. Rev. D* **60**, 034509 (1999) [arXiv:hep-lat/9901004].
[18] H. B. Meyer and M. J. Teper, *Phys. Lett. B* **605** (2005) 344 [arXiv:hep-ph/0409183]. H. B. Meyer, arXiv:hep-lat/0508002.
[19] Y. Chen *et al.*, *Phys. Rev. D* **73** (2006) 014516 [arXiv:hep-lat/0510074].
[20] B. Lucini and M. Teper, *JHEP* **0106**, 050 (2001) [arXiv:hep-lat/0103027].
[21] C. J. Morningstar and M. J. Peardon, *Phys. Rev. D* **56** (1997) 4043 [arXiv:hep-lat/9704011].
[22] H. B. Meyer, arXiv:0808.3151 [hep-lat].
[23] W. J. Lee and D. Weingarten, *Phys. Rev. D* **61** (2000) 014015 [arXiv:hep-lat/9910008].
[24] C. McNeile and C. Michael [UKQCD Collaboration], *Phys. Rev. D* **63** (2001) 114503 [arXiv:hep-lat/0010019].
[25] W. A. Bardeen, A. Duncan, E. Eichten, N. Isgur and H. Thacker, *Phys. Rev. D* **65** (2001) 014509 [arXiv:hep-lat/0106008].
[26] C. Michael, *Nucl. Phys. B* **327** (1989) 515.
[27] J. Sexton, A. Vaccarino and D. Weingarten, *Phys. Rev. Lett.* **75** (1995) 4563 [arXiv:hep-lat/9510022].
[28] L. Burakovsky and P. R. Page, *Phys. Rev. D* **59** (1999) 014022 [Erratum-ibid. D **59** (1999) 079902] [arXiv:hep-ph/9807400].
[29] A. Chodos, R. L. Jaffe, K. Johnson, C. B. Thorn and V. F. Weisskopf, *Phys. Rev. D* **9** (1974) 3471.
[30] A. Chodos, R. L. Jaffe, K. Johnson and C. B. Thorn, *Phys. Rev. D* **10** (1974) 2599.
[31] J. F. Donoghue, K. Johnson and B. A. Li, *Phys. Lett. B* **99** (1981) 416.
[32] C. E. Carlson, T. H. Hansson and C. Peterson, *Phys. Rev. D* **27** (1983) 1556.
[33] T. H. Hansson, K. Johnson and C. Peterson, *Phys. Rev. D* **26** (1982) 2069.
[34] C. E. Carlson, T. H. Hansson and C. Peterson, *Phys. Rev. D* **30** (1984) 1594.
[35] M. S. Chanowitz and S. R. Sharpe, Nucl. Phys. B **222** (1983) 211 [Erratum-ibid. B **228** (1983) 588].
[36] D. Robson, *Z. Phys. C* **3** (1980) 199.
[37] N. Isgur and J. E. Paton, *Phys. Rev. D* **31** (1985) 2910.
[38] J. M. Cornwall, *Phys. Rev. D* **26** (1982) 1453.
[39] C. W. Bernard, *Phys. Lett. B* **108** (1982) 431.
[40] J. F. Donoghue, *Phys. Rev. D* **29** (1984) 2559.
[41] J. M. Cornwall and A. Soni, *Phys. Lett. B* **120** (1983) 431.
[42] C. N. Yang, *Phys. Rev.* **77** (1950) 242.
[43] M. Jacob and G. C. Wick, *Annals Phys.* **7** (1959) 404 [*Annals Phys.* **281** (2000) 774].
[44] T. Barnes, *Z. Phys. C* **10** (1981) 275.
[45] V. Mathieu, F. Buisseret and C. Semay, *Phys. Rev. D* **77** (2008) 114022 [arXiv:0802.0088 [hep-ph]].
[46] F. Brau and C. Semay, *Phys. Rev. D* **70** (2004) 014017 [arXiv:hep-ph/0412173].
[47] A. Szczepaniak, E. S. Swanson, C. R. Ji and S. R. Cotanch, *Phys. Rev. Lett.* **76** (1996) 2011 [arXiv:hep-ph/9511422]. A. P. Szczepaniak and E. S. Swanson, *Phys. Lett. B* **577** (2003) 61 [arXiv:hep-ph/0308268].
[48] G. S. Bali, *Phys. Rev. D* **62** (2000) 114503 [arXiv:hep-lat/0006022].
[49] T. Schafer and E. V. Shuryak, *Phys. Rev. Lett.* **75** (1995) 1707 [arXiv:hep-ph/9410372].
[50] A. B. Kaidalov and Yu. A. Simonov, *Phys. Atom. Nucl.* **63** (2000) 1428 [*Yad. Fiz.* **63** (2000) 1428] [arXiv:hep-ph/9911291].
[51] A. B. Kaidalov and Yu. A. Simonov, *Phys. Lett. B* **636** (2006) 101 [arXiv:hep-ph/0512151].
[52] V. Mathieu, C. Semay and F. Brau, *Eur. Phys. J. A* **27** (2006) 225 [arXiv:hep-ph/0511210].
[53] M. Cardoso and P. Bicudo, arXiv:0807.1621 [hep-lat].
[54] W. S. Hou and A. Soni, *Phys. Rev. D* **29** (1984) 101.

[55] F. J. Llanes-Estrada, P. Bicudo and S. R. Cotanch, *Phys. Rev. Lett.* **96** (2006) 081601 [arXiv:hep-ph/0507205].
[56] V. Mathieu, C. Semay and B. Silvestre-Brac, *Phys. Rev. D* **74** (2006) 054002 [arXiv:hep-ph/0605205].
[57] V. Mathieu, C. Semay and B. Silvestre-Brac, *Phys. Rev. D* **77** (2008) 094009 [arXiv:0803.0815 [hep-ph]].
[58] J. M. Maldacena, *Adv. Theor. Math. Phys.* **2** (1998) 231 [*Int. J. Theor. Phys.* **38** (1999) 1113] [arXiv:hep-th/9711200].
[59] E. Witten, *Adv. Theor. Math. Phys.* **2** (1998) 505 [arXiv:hep-th/9803131].
[60] C. Csaki, H. Ooguri, Y. Oz and J. Terning, *JHEP* **9901** (1999) 017 [arXiv:hep-th/9806021].
[61] R. C. Brower, S. D. Mathur and C. I. Tan, *Nucl. Phys. B* **587** (2000) 249 [arXiv:hep-th/0003115].
[62] H. Boschi-Filho and N. R. F. Braga, *JHEP* **0305** (2003) 009 [arXiv:hep-th/0212207].
[63] H. Boschi-Filho, N. R. F. Braga and H. L. Carrion, *Phys. Rev. D* **73** (2006) 047901 [arXiv:hep-th/0507063].
[64] M. J. Teper, [arXiv:hep-lat/9711011].
[65] R. L. Jaffe, K. Johnson and Z. Ryzak, *Annals Phys.* **168** (1986) 344.
[66] M. Shifman, A.I. Vainshtein and V.I. Zakharov, *Nucl. Phys. B***147** (1979) 385; ibid 448; V. A. Novikov, M. A. Shifman, A. I. Vainshtein and V. I. Zakharov, *Nucl. Phys. B* **165**, 67 (1980).
[67] E. V. Shuryak, *Nucl. Phys. B* **203**, 116 (1982).
[68] A. l. Zhang and T. G. Steele, *Nucl. Phys. A* **728**, 165 (2003) [arXiv:hep-ph/0304208].
[69] S. Narison, *Phys. Rev. D* **73**, 114024 (2006) [arXiv:hep-ph/0512256].
[70] J. I. Latorre, S. Narison and S. Paban, *Phys. Lett. B* **191**, 437 (1987).
[71] G. Hao, C. F. Qiao and A. L. Zhang, *Phys. Lett. B* **642**, 53 (2006) [arXiv:hep-ph/0512214].
[72] L. J. Reinders, H. Rubinstein and S. Yazaki, *Phys. Rept.* **127** (1985) 1.
[73] B. V. Geshkenbein and B. L. Ioffe, *Nucl. Phys. B* **166**, 340 (1980).
[74] A. E. Dorokhov and N. I. Kochelev, *Z. Phys. C* **46**, 281 (1990).
[75] T. Schafer and E. V. Shuryak, *Rev. Mod. Phys.* **70**, 323 (1998) [arXiv:hep-ph/9610451].
[76] H. J. Lee, N. I. Kochelev and V. Vento, *Phys. Lett. B* **610**, 50 (2005)
[77] H. J. Lee, N. I. Kochelev and V. Vento, *Phys. Rev. D* **73**, 014010 (2006)
[78] H. J. Lee and N. I. Kochelev, *Phys. Lett. B* **642**, 358 (2006).
[79] A. E. Dorokhov, N. I. Kochelev and Yu. A. Zubov, *Int. J. Mod. Phys. A* **8** (1993) 603.
[80] D. Diakonov, *Prog. Part. Nucl. Phys.* **51**, 173 (2003)
[81] N. I. Kochelev, *Phys. Part. Nucl.* **36**, 608 (2005) [*Fiz. Elem. Chast. Atom. Yadra* **36**, 1157 (2005)].
[82] B. L. Ioffe, *Prog. Part. Nucl. Phys.* **56**, 232 (2006).
[83] M. D'Elia, A. Di Giacomo and E. Meggiolaro, *Phys. Lett. B* **408** (1997) 315 [arXiv:hep-lat/9705032].
[84] A. A. Migdal and M. A. Shifman, *Phys. Lett. B* **114** (1982) 445.
[85] J. R. Ellis and J. Lanik, *Phys. Lett. B* **150** (1985) 289.
[86] G. B. West, arXiv:hep-ph/9608258; G.B. West, *Phys. Rev. Lett.* **77** (1996) 2622; *Nucl. Phys.* (Proc. Suppl.) **54**A (1997) 353.
[87] V. Vento, *Phys. Rev. D* **73** (2006) 054006 [arXiv:hep-ph/0401218].
[88] C. A. Dominguez and N. Paver, *Z. Phys. C* **31** (1986) 591.
[89] J. Bordes, V. Giminez and J. A. Penarrocha, *Phys. Lett. B* **223** (1989) 251.
[90] L. S. Kisslinger and M. B. Johnson, *Phys. Lett. B* **523** (2001) 127 [arXiv:hep-ph/0106158].
[91] S. Narison, *Nucl. Phys. Proc. Suppl.* **121** (2003) 131 [arXiv:hep-ph/0208081].
[92] H. G. Dosch and S. Narison, *Nucl. Phys. Proc. Suppl.* **121** (2003) 114 [arXiv:hep-ph/0208271].
[93] H. Forkel, *Phys. Rev. D* **71**, 054008 (2005) [arXiv:hep-ph/0312049].
[94] P. Pascual and R. Tarrach, *Phys. Lett. B* **113**, 495 (1982).
[95] H. Forkel, *Phys. Rev. D* **64**, 034015 (2001) [arXiv:hep-ph/0005004].
[96] D. Harnett and T. G. Steele, *Nucl. Phys. A* **695**, 205 (2001) [arXiv:hep-ph/0011044].
[97] N. Kochelev and D. P. Min, *Phys. Rev. D* **72**, 097502 (2005)
[98] M. C. Tichy and P. Faccioli, arXiv:0711.3829 [hep-ph].
[99] D. Harnett, K. Moats and T. G. Steele, arXiv:0804.2195 [hep-ph].
[100] S. Narison, *Nucl. Phys. B* **509**, 312 (1998) [arXiv:hep-ph/9612457].
[101] S. Narison, Nucl. Phys. A **675** (2000) 54C [arXiv:hep-ph/9909470].
[102] P. R. Page, arXiv:hep-ph/0107016.
[103] $\overline{\mathrm{P}}$ANDA Collaboration: http:/www-panda.gsi.de/ .
[104] D. Robson, *Nucl. Phys. B* **130** (1977) 328.
[105] D. M. Asner *et al.*, arXiv:0809.1869; BES Collaboration : http://bes.ihep.ac.cn/ .
[106] N. I. Kochelev, arXiv:hep-ph/9902203.
[107] GlueX Collaboration: http://www.gluex.org/ .
[108] A. A. Natale, *Phys. Lett. B* **362** (1995) 177 [arXiv:hep-ph/9509280].
[109] A. J. Schramm, *J. Phys. G* **25** (1999) 1965 [arXiv:hep-ph/9907217].
[110] M. Bashkanov, *AIP Conf. Proc.* **619** (2002) 525.
[111] M. Chanowitz, *Phys. Rev. Lett.* **95** (2005) 172001 [arXiv:hep-ph/0506125].
[112] K. T. Chao, X. G. He and J. P. Ma, *Phys. Rev. Lett.* **98** (2007) 149103 [arXiv:0704.1061 [hep-ph]].
[113] M. S. Chanowitz, *Phys. Rev. Lett.* **98** (2007) 149104 [arXiv:0704.1616 [hep-ph]].
[114] R. L. Jaffe, *Phys. Rev. D* **15** (1977) 267.
[115] C. Amsler and F. E. Close, *Phys. Rev. D* **53** (1996) 295 [arXiv:hep-ph/9507326].
[116] A. Abele *et al.* [Crystal Barrel Collaboration], *Eur. Phys. J. C* **19** (2001) 667.

[117] E. V. Shuryak, *Phys. Rept.* **61** (1980) 71.
[118] Nucl. Phys. A 757 (2005) 1- 283, *First three years of operation of RHIC.*
[119] E. V. Shuryak and I. Zahed, *Phys. Rev. D* **70** (2004) 054507 [arXiv:hep-ph/0403127].
[120] C. S. Gao, X. Q. Li and W. Lu, *Phys. Rev. C* **52** (1995) 421.
[121] S. Kabana and P. Minkowski, *Phys. Lett. B* **472** (2000) 155 [arXiv:hep-ph/9907570].
[122] P. Minkowski, S. Kabana and W. Ochs, arXiv:hep-ph/0011040.
[123] I. N. Mishustin, L. M. Satarov and W. Greiner, *J. Phys. G* **32** (2006) L59 [arXiv:hep-ph/0606251].
[124] V. Koch, A. Majumder and J. Randrup, *Phys. Rev. Lett.* **95** (2005) 182301 [arXiv:nucl-th/0505052].
[125] F. Karsch, S. Ejiri and K. Redlich, *Nucl. Phys. A* **774** (2006) 619 [arXiv:hep-ph/0510126].
[126] C. Ratti, S. Roessner, M. A. Thaler and W. Weise, *Eur. Phys. J. C* **49** (2007) 213 [arXiv:hep-ph/0609218].
[127] N. Kochelev and D. P. Min, *Phys. Lett. B* **650** (2007) 239 [arXiv:hep-ph/0611250].
[128] D. E. Miller, *Phys. Rept.* **443** (2007) 55 [arXiv:hep-ph/0608234].
[129] V. Vento, *Phys. Rev. D* **75** (2007) 055012 [arXiv:hep-ph/0609219].
[130] J. Sollfrank and U. Heinz, *Z. Phys.* **C65** (1995) 111; A. Drago, M. Gibilisco and C. Ratti, *Nucl. Phys.* **A742** (2004) 165; B.-J. Schaefer, O. Bohr and J. Wambach, *Phys. Rev.* **D65** (2002) 105008.
[131] S. Wicks and M. Gyulassy, *J. Phys. G* **34** (2007) S989 [arXiv:nucl-th/0701088].
[132] B. Muller and J. L. Nagle, *Ann. Rev. Nucl. Part. Sci.* **56** (2006) 93 [arXiv:nucl-th/0602029].
[133] B. Alles, M. D'Elia and A. Di Giacomo, *Nucl. Phys. B* **494** (1997) 281 [Erratum-ibid. B **679** (2004) 397] [arXiv:hep-lat/9605013].
[134] A. Peshier, *Phys. Rev. Lett.* **97** (2006) 212301 [arXiv:hep-ph/0605294].
[135] C. Amsler and F.E. Close, *Phys. Lett. B* **353** (1995) 385 ; F.E. Close and A. Kirk, *Phys. Lett. B* **483** (2000) 345 .
[136] F.E. Close and Q. Zhao, *Phys. Rev. D* **71** (2005) 094022.
[137] C. Amsler *et al.*, *Phys. Lett. B* **342** (1995) 433 ; Phys. Lett. B **340** (1994) 259.
[138] C. Michael and M. Teper, *Nucl. Phys. B* **314**, 347 (1989).
[139] X.G. He, X.Q. Li, X. Liu, and X.Q. Zeng, *Phys. Rev. D* **73** (2006) 051502 ; *ibid.* D **73** (2006) 114026.
[140] H. Y. Cheng, C. K. Chua and K. F. Liu, *Phys. Rev. D* **74** (2006) 094005 [arXiv:hep-ph/0607206].
[141] N. Mathur *et al.*, *Phys. Rev. D* **76** (2007) 114505 [arXiv:hep-ph/0607110].
[142] K. T. Chao, X. G. He and J. P. Ma, *Eur. Phys. J. C* **55** (2008) 417 [arXiv:hep-ph/0512327].
[143] S. B. Gerasimov, M. Majewski and V. A. Meshcheryakov, arXiv:0708.3762 [hep-ph].
[144] In refs. [70, 71] three-gluon interpolating currents were used for the scalar and pseudoscalar glueballs.
[145] Some examples of Borel transformations are $\hat{B}\left(\frac{1}{p^2-\alpha}\right)^{\beta} = (-1)^{\beta}(M^2)^{1-\beta}\frac{e^{-\alpha/M^2}}{(\beta-1)!}$, $\hat{B}\left((p^2)^m \ln(-p^2)\right) = -m!(M^2)^{m+1}$ and $\hat{B}\left((p^2)^m\right) = 0$, for $m \geq 0$.
[146] The importance of the quark loop contributions to the spin-zero gluonic correlators arising from instanton-antiinstanton configurations has been demonstrated in refs. [49, 98].